Review in Advance first posted online on April 3, 2017. (Changes may still occur before final publication online and in print.)

Deformation of Crystals: Connections with Statistical Physics

James P. Sethna,[1] Matthew K. Bierbaum,[1] Karin A. Dahmen,[2] Carl P. Goodrich,[3] Julia R. Greer,[4] Lorien X. Hayden,[1] Jaron P. Kent-Dobias,[1] Edward D. Lee,[1] Danilo B. Liarte,[1] Xiaoyue Ni,[4] Katherine N. Quinn,[1] Archishman Raju,[1] D. Zeb Rocklin,[1] Ashivni Shekhawat,[5] and Stefano Zapperi[6,7]

[1]Laboratory of Atomic and Solid State Physics, Cornell University, Ithaca, New York 14853-2501; email: sethna@lassp.cornell.edu

[2]Physics Department, University of Illinois at Urbana-Champaign, Urbana, Illinois 61810

[3]School of Engineering and Applied Sciences, Harvard University, Cambridge, Massachusetts 02138

[4]Division of Engineering and Applied Sciences, California Institute of Technology, Pasadena, California 91125

[5]Materials Sciences Division, Lawrence Berkeley National Laboratory, Berkeley, California 94720

[6]Department of Physics and Center for Complexity and Biosystems, University of Milano, 20133 Milano, Italy

[7]Institute for Scientific Interchange Foundation, 10126 Torino, Italy

Annu. Rev. Mater. Res. 2017. 47:14.1–14.30

The *Annual Review of Materials Research* is online at matsci.annualreviews.org

https://doi.org/10.1146/annurev-matsci-070115-032036

Keywords

plasticity, crystals, critical phenomena, irreversible deformation, dislocation, work hardening, renormalization group

Abstract

We give a bird's-eye view of the plastic deformation of crystals aimed at the statistical physics community, as well as a broad introduction to the statistical theories of forced rigid systems aimed at the plasticity community. Memory effects in magnets, spin glasses, charge density waves, and dilute colloidal suspensions are discussed in relation to the onset of plastic yielding in crystals. Dislocation avalanches and complex dislocation tangles are discussed via a brief introduction to the renormalization group and scaling. Analogies to emergent scale invariance in fracture, jamming, coarsening, and a variety of depinning transitions are explored. Dislocation dynamics in crystals challenge nonequilibrium statistical physics. Statistical physics provides both cautionary tales of subtle memory effects in nonequilibrium systems and systematic tools designed to address complex scale-invariant behavior on multiple length scales and timescales.

1. PLASTIC DEFORMATION OF MATERIALS: WHAT IS DIFFERENT?

Stress: force per unit area σ applied to a crystal. Both ϵ and σ are tensors, a fact we largely ignore

Strain: fractional amount ϵ a crystal is stretched or sheared, twisted, or compressed

Equilibrium: in this article, equilibrium and nonequilibrium ordinarily refer to thermal equilibrium (see sidebar titled Equilibrium Statistical Mechanics below); most of our systems reach mechanical equilibrium—a metastable state

Many of us, when trying to scoop ice cream, have induced plastic deformation: The spoon remains bent (see **Figure 1** and sidebar titled Bent Spoon and Yield Stress). Speculations about strategies for understanding our bent spoon represent the topic of this review.

The physics and engineering communities have historically focused on studying how plastic deformation is similar to simpler systems. Elastic materials respond to stress fields via strain fields, liquids respond via viscous strain rates, and complex fluids are often describable via frequency-dependent viscoelastic responses. Many properties of crystals, magnets, liquid crystals, superconductors, superfluids, and field theories of the early universe can be described by focusing on long length scales and assuming that the materials are locally close to equilibrium. Physicists use generalized hydrodynamics (1, 2; 3, pp. 37–136) or Landau theory (4) and have systematized how conserved quantities (particle number, momentum, energy) and broken symmetries (magnetization, crystalline order) are assembled into order parameter fields. Engineers apply continuum field theories (5) using phenomenological materials models to study materials behavior. They incorporate state variables like dislocation density, yield stress, or texture to describe the behavior of real materials at macroscopic scales. These models have been effectively incorporated into the computational frameworks used to design everything from spoons to airplanes. In Section 2 we provide a physicist's introduction to the challenges posed by plasticity in metals, discussing or ignoring many crucial features (slip systems, partial dislocations, grain boundaries, etc.) but emphasizing how the broken translational symmetry of crystals makes them unusual among condensed matter systems.

Figure 1
Bent spoon and yield stress.

BENT SPOON AND YIELD STRESS

A metal spoon will spring back into its original shape under ordinary use, but when scooping hard ice cream, one may bend the spoon too far for it to recover. The spoon is made up of many crystalline grains, each of which has a regular grid of atoms. To permanently deform the spoon, atomic planes must slide past one another. Such glide happens through the motion of dislocation lines. The dynamics, interactions, and entanglement of these dislocation lines form the microscopic underpinnings of crystal plasticity, inspiring this review.

Inspired by the plasticity and failure of practical materials, the statistical physics community has studied a remarkable variety of rigid nonequilibrium systems evolving under stress. They have focused on what makes these systems different—how magnets, sand, and other rigid systems under external stress behave in qualitatively different ways from simpler systems (6). This article summarizes results from many of these studies, from magnetic hysteresis to jamming of granular materials, in brief vignettes similar to the one shown in **Figure 1**.

Striking regularities that emerge in the deformation and failure of materials lure us to search for a systematic theory. First, despite a bewildering variety of materials morphologies, most structural materials share certain characteristic damage thresholds. Plastic deformation in practical materials does not arise at arbitrarily small applied stresses: The onset of deformation characterizes the yield strength of materials (see **Figure 3** below). The yield stress is an approximation; creep and fatigue allow for hysteretic changes below the yield stress. But by ignoring certain physical mechanisms (e.g., things like vacancy diffusion and cross slip that typically go away at low temperatures), we can study a theory that predicts a sharp threshold in quasi-static deformations and that hence provides an effective explanation of the observed, but less sharp, transitions in practical materials.

The yield stress represents the division between elastic and plastic, the division between reversible and hysteretic macroscopic deformations. Fundamentally, equilibrium systems forget their history: All other microscopic degrees of freedom are slaves to the state variables. The chaotic local dynamics on the atomic scale scramble the history of how the material was prepared; only those quantities preserved by the dynamics can matter for the long-time macroscopic behavior. In contrast, plastically deformed materials are not in local equilibrium, and their properties depend on their history. The blacksmith hammering the red-hot horseshoe and quenching it into water is altering a complex microstructure that governs its toughness and strength; a cast-iron horseshoe of identical chemical composition could be brittle. In Section 3 we briefly and broadly review how the history of deformation has been reflected in other statistical mechanics contexts: Can the memory of a material's past be effectively summarized in a finite number of continuum variables? What can we glean from these other systems about what might be special about the dislocation configurations left behind after yielding and unloading in crystals?

Statistical physicists adore power laws and emergent scale invariance; when systems appear the same on different scales, we have powerful, systematic tools by which to quantitatively predict the resulting behavior. In Section 4 we examine evidence that dislocation evolution and plastic flow exhibit just this kind of scale invariance—power-law distributions of dislocation avalanches and complex, perhaps scale-invariant morphologies. We discuss plasticity models that explain this scale invariance as self-organized criticality, controlled by work hardening, and also discuss the possibility that these effects are due to a proximity to a critical failure stress. We discuss the theoretical renormalization group framework that has been used to analyze emergent scale invariance, introduce related nonequilibrium statistical mechanics systems that have been studied using these methods, and speculate about possible connections to plastic deformation in crystals. We then also discuss the tension between the universality traditionally expected at critical points and the strong nonuniversal dependence on materials, morphology, and loading seen at the yielding transition.

Slip systems: the set of slip planes for the low-energy Burgers vectors for a given crystal symmetry. The initial deformation of pure metals usually activates only one or a few slip systems

Slip plane: the plane accessible to a dislocation of a given Burgers vector via glide

Burgers vector: topological charge of a dislocation: number of extra planes of atoms crossed when encircling the defect (7, Section 9.4]

Partial dislocations: the edge of a stacking fault, often forming the core of a dislocation, described by fractions of a Burger's vector

Stacking fault: for simple fcc metals, a deviation from the fcc ABCABC stacking—typically low energy, because the nearest-neighbor structures are unchanged

Rigid: Rigid systems have an energy cost to deforming some continuum field – magnetic, elastic, charge density distortion, superfluid, . . .

2. PLASTICITY: A PHYSICIST'S INTRODUCTION

Almost any collection of atoms or molecules, when cooled, will form into a rigid, solid object. This rigidity is an unappreciated, profound state of matter. Much is made of the precision measurements made possible by the Josephson effect in superconductors or the quantum Hall effect in two-dimensional electron gases. But the rigidity of solids underlies almost every measurement we do. For example, it allows the mirrors of LIGO to be held multiple kilometers apart with an accuracy

Creep: dislocation motions, like dislocation climb, that proceed slowly and remain present below the traditional yield stress. They are usually thermally activated. Creep is a component of rate-dependent plasticity

Cross slip: the motion of the screw portion of a dislocation loop into a different glide plane, often involving thermally activated restructuring of partial dislocations

much smaller than an atomic nucleus. From bridges to bones, the rigidity of solids underpins our world.

Rigidity may seem straightforward. Atoms and molecules bond together, and breaking bonds demands energy—either thermal energy to melt the material or external forces to bend, shear, or fracture it. For glasses and amorphous materials, the key question is what makes them different from liquids. Structurally similar to liquids, how and why do such materials get trapped into a subset of the possible atomic configurations? What is the nature of the glass transition, at which the material stops flowing and develops an elastic rigidity to small external forces? We touch upon current jamming theories regarding the rigidity of glasses in **Figure 15** below.

Even the rigidity of crystals is subtle. Each atom in a crystal knows its place: The regular array of atoms cannot flow. A crystal has no linear shear-rate response to an external strain of the crystalline lattice (see **Figure 2*a*,*b*** and sidebar titled Crystalline Rigidity). But it will shear under high loads, plastically deforming through the motion of dislocations (see **Figure 2*c*,*d*** and sidebar titled Crystalline Rigidity). What divides elastic from plastic?

How far can one strain a crystal before it will plastically deform—rearranging its lattice to lower its energy? It is easy to see, but quite surprising, that the limiting stability region of an equilibrium crystal is microscopic. Consider a crystal being compressed vertically (see **Figure 2*c*,*d*** and sidebar titled Crystalline Rigidity), with free boundary conditions along the horizontal. It is clear that the lowest free energy configuration of the crystal will change—removing one horizontal plane

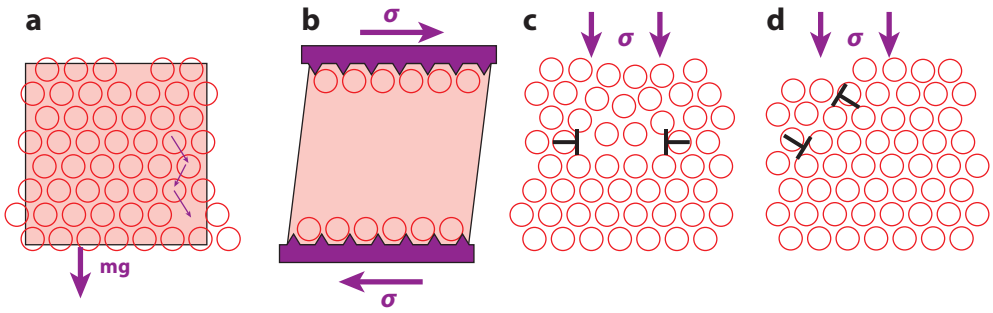

Figure 2

Crystalline rigidity. Under the action of external stress, crystals can exhibit (*a*) liquid-like, (*b*) solid-like, or (*c*,*d*) plastic responses.

CRYSTALLINE RIGIDITY

In **Figure 2*a***, under a force such as gravity that couples to the mass density, an equilibrium crystal can flow like a liquid at a rate linear in the gravitational force, via vacancy diffusion. [This is true at temperatures above the roughening transition (8), at which all the equilibrium surfaces have steps that can absorb and emit vacancies.] In **Figure 2*b***, crystals are rigid to shears σ that couple to the lattice (i.e., the broken translational symmetry). In **Figure 2*c***, a crystal sheared or compressed more than half a lattice constant will, in equilibrium, lose a plane of atoms. Here a dislocation loop surrounds a disk of missing atoms, which can grow only by climb, again via thermally activated vacancy diffusion. In **Figure 2*d***, the dominant shear relaxation at low temperatures is glide, whereby a dislocation loop can grow along a slip plane to relieve stress without involving vacancies (see **Figure 7*a*** below). The nucleation rate for the dislocation loops in panels *c* and *d* of **Figure 2** goes to zero faster than linearly as the compression goes to zero; there is no linear viscous flow response to forces that couple to the lattice. This behavior distinguishes crystals from liquids.

of atoms and moving them to the edge—once the compressive deformation reaches a lattice constant. Similarly, a bent crystal can lower its energy by developing a low-angle grain boundary once the net deformation is of order the lattice constant times the logarithm of the number of atomic layers. This is quite different from most broken symmetry systems; magnets, superfluids, and superconductors can be twisted at their edges by large angles or phases before they prefer to generate defects to relax. Crystalline rigidity is frail.[1]

This frailty is not just a theoretical curiosity. Although perfect single crystals (such as nanowhiskers) can support enormous strains before yielding, high-quality, nearly perfect fcc crystals have very low thresholds for plastic deformation. Consider a dislocation line segment in a crystal, pinned at two points a distance L apart, perhaps by inclusions, impurities, or other dislocations. (We ignore effects due to the discreteness of the crystalline lattice.) The component of the external stress σ that couples to the dislocation will cause it to bow out, forming a roughly circular arc, until its line tension and interaction energy balance the external stress at a rough curvature diameter $D_c(\sigma)$. When $D_c < L$, the loop grows without bound, sometimes pinching off to form a growing dislocation loop.

The durable crystals familiar to us have rather large densities of pinning sites, often arising from the tangle of dislocations formed by previous plastic deformation. There is an energy barrier impeding the crossing of two [or more (12)] dislocations;[2] they often instead merge into dislocation junctions, which act as pinning points. If the density of dislocation lines crossing a unit area is ρ, a dislocation passing through the tangle will typically have pinning intersection points separated by $L \sim 1/\sqrt{\rho}$ (see **Figure 3*a*** and sidebar titled Dislocation Pinning and Work Hardening). This implies a yield stress $\sigma_Y \propto \sqrt{\rho}$—the Taylor relation (13).[3] This power-law scaling relation, although simply derived, foreshadows the types of predictions derived from emergent scale invariance in Section 4.

As plastic deformation proceeds, the dislocation lines stretch and multiply, increasing their density and further increasing the yield stress. This work hardening makes plastic deformation self-limiting in crystals; a weak spot becomes stronger when it yields.[4] Hence a pristine copper wire (or an ordinary metal clothes hanger) can be bent quite easily into a tight curve. But once bent, it becomes far more resistant to further deformation; bending takes far less force than unbending.

Plastic deformation is the study of the nonequilibrium collective dynamics of spatially extended topological defect lines, with long-range elastic interactions and complex constraints on the defect motions. Each of these features has separately become a focus of statistical physics in the past decades. Indeed, many of us have been inspired to study memory effects and critical phenomena in these other systems because of seeming relations to the challenging practical problems illustrated by bent spoons. Let us now proceed with a distillation of some of the key ideas developed in statistical physics that could be useful or inspirational for the study of plastic deformation of crystals.

3. MEMORY AND STATE VARIABLES

It is a truism in metallurgy that the mechanical properties of crystals depend on their thermal and deformation history—the heating and beating suffered by the material in the past (16).

[1] Smectic liquid crystals—made of stacked two-dimensional liquid layers—are also frail (9).

[2] There is no topological reason to prevent dislocations from crossing (Reference 7, chapter 9), although often a jog will be left behind, which then can impede glide.

[3] One must note that grain boundaries can also act as pinning sites for dislocations, but the yield stress for grains of size L does not scale as $1/L$, but approximately as $1/\sqrt{L}$ (the Hall-Petch relation), due to the need for several dislocations to cooperate in punching the lead dislocation through the wall (e.g., in a dislocation pileup). This different scaling will be a challenge to scaling theories like those discussed in Section 4.

[4] Metallic glasses, in contrast, become weaker as they shear, leading to failure via slip bands (14, 15).

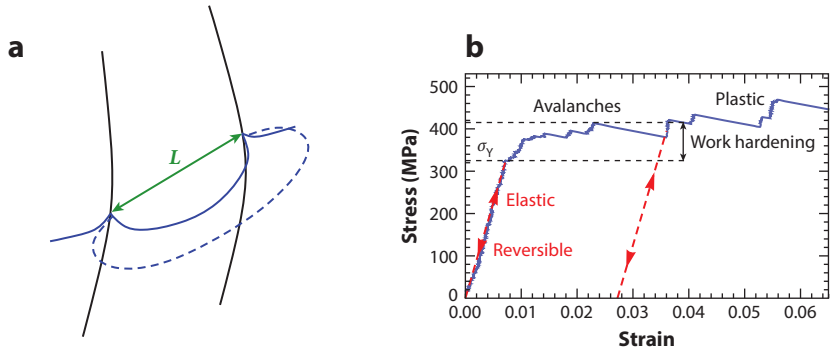

Figure 3

(*a*) Pinned dislocation line. (*b*) Avalanches and work hardening in a micropillar stress-strain curve.

DISLOCATION PINNING AND WORK HARDENING

In **Figure 3*a***, dislocations get pinned on other dislocations, dirt, inclusions, or their own jogs. Under stress, they will bow out reversibly, with a curvature diameter that shrinks roughly linearly with increasing stress, until it becomes less than the distance L between pins. At that point, the dislocation balloons out and triggers an avalanche. This argument explains the observed scaling of the yield stress $\sigma_Y \sim 1/L$, with the distance L between pinning points (see, e.g., Reference 11, chapter 10). In **Figure 3*b***, micropillar deformation, showing avalanches (X. Ni & J.R. Greer, unpublished data). The response of a material is reversible below a yield stress σ_Y, after which dislocation avalanches lead to plastic deformation. When unloaded, the material will respond reversibly until reloaded to roughly the previous maximum stress. Subsequent plastic flow increases the length and density of dislocations, leading to more pinning and work hardening.

Mechanical plastic deformation of a crystal typically increases the threshold for further deformation (work hardening); heating it to high temperatures anneals the crystal back to a plastically soft state. As discussed in Section 2, different theories of plasticity attempt to encapsulate this history dependence into a variety of state variables. The simple sample yield stress we discuss above could be promoted, for example, to a spatially dependent yield stress of an inhomogeneously processed specimen; to an entire yield surface in the six-dimensional space of stresses; or to a scalar-, tensor-, or slip system–specific dislocation density.

The history dependence of other rigid systems has been an active field in statistical mechanics. Some investigators have focused on how nonequilibrium systems might be similar to equilibrium phases, with a thermodynamics resulting from a guiding principle similar to maximizing entropy. Some have explored the weird ways in which particular rigid systems respond to external forcing. And some have focused on how nonequilibrium systems might be governed by critical points (Section 4), with scaling behavior similar to those of continuous equilibrium phase transitions.

The plasticity of crystals forms the prototypical example of a nonequilibrium, history-dependent rigid system. It has inspired and guided careful work on memory effects in other statistical mechanical contexts. We may hope that some of the unusual memory ramifications observed in these simpler systems are relevant for plasticity. In this section, we briefly highlight studies of the first two types (nonequilibrium thermodynamics versus weird memory effects) and

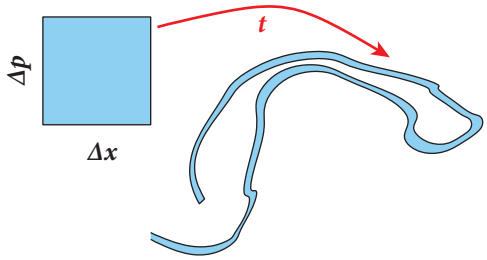

Figure 4

Liouville's theorem: the volume in the box is the same as the volume in the spaghetti.

EQUILIBRIUM STATISTICAL MECHANICS

Equilibrium systems are simple (see Reference 7, chapter 4) first because their dynamics is chaotic (a compact region, shown in **Figure 4**, becomes stretched and twisted). Chaotic systems rapidly lose all information about their previous state, except for conserved quantities (energy, volume, number of particles, etc.) and fields associated with broken symmetries (magnetization, crystalline strain, superfluid phase, etc.). Their time-averaged behavior then becomes a weighted average over their attractor. Thermal equilibrium systems are also simple because their energy-conserving Hamiltonian dynamics preserve volume in phase space (Liouville's theorem), telling us that the attractor includes all possible states consistent with the preserved information, weighted by phase space volume (a maximum-entropy state). This property leads directly to free energies and thermodynamics. Temperature, pressure, chemical potential, and stress arise as Lagrange multipliers to constrain the conserved energy, volume, number, and strain.

discuss how they might give insight into practical plasticity problems. We consider nonequilibrium critical points in Section 4.

Edwards & Oakeshott (18) proposed the most influential recent analogy between nonequilibrium systems and equilibrium statistical mechanics (see **Figure 4** and sidebar titled Equilibrium Statistical Mechanics): a thermodynamic theory of packed granular powders.[5] Edwards & Oakeshott posited a phase space of force-balanced jammed arrangements of grains producing a kind of granular entropy, with volume replacing energy as the conserved quantity and temperature replaced by a compactivity field. Recent experiments (17, 20) (see **Table 1** and sidebar titled Compactivity Versus Angoricity) show very generally that such a description does not satisfy the zeroth law (two kinds of particles in equilibrium with a third must be in equilibrium with one another). Indeed, it is hard to see how the admittedly complicated dynamics of grain motion as the system is tamped or sheared would rearrange particles to transmit extra volume effectively through that system. However, the forces between touching particles can rearrange dramatically under changing loads, even for fixed particle contacts. [Puckett & Daniels (24) mention that forces and torques balance at each contact, whereas volume is merely conserved globally.] This could perhaps form the basis of a thermodynamic theory (see **Table 1** and sidebar titled Compactivity Versus Angoricity).

There are serious challenges to similar analogies between dislocations and equilibrium statistical mechanics. Dislocation energies are strongly coupled to their atomic environments; they

[5] Note that low-density shaken granular materials fluidize; such systems do explore their available states and in many regimes can be approximated well by theories drawing from thermodynamics (23).

Table 1 A few properties of Boltzmann, Edwards, and HC-EB ensembles

	Boltzmann	Edwards	HC-EB
Conserved quantity	Energy, E	Volume, V	Force moment, $\hat{\Sigma}$
Entropy	$S = k_B \ln \Omega_B(E)$	$S = \lambda \ln \Omega(V)$	$S = \lambda \ln \Omega(\hat{\Sigma})$
Intensive quantity	Temperature	Compactivity	Angoricity
	$\frac{1}{T} = \frac{\partial S(E)}{\partial E}$	$\frac{1}{X} = \frac{\partial S(V)}{\partial V}$	$\alpha_{\mu\lambda} = \frac{\partial S(\Sigma_{\mu\lambda})}{\partial \Sigma_{\mu\lambda}}$
Distribution	$\exp[-E/(k_B T)]$	$\exp(-V/X)$	$\exp(-\alpha_{\mu\lambda} \cdot \Sigma_{\mu\lambda})$

COMPACTIVITY VERSUS ANGORICITY

There has been an ambitious attempt to use statistical mechanics to derive a thermodynamics of dry grains and dense, non-Brownian suspensions (17). Grains of sand do not move unless pushed; energy and temperature are unimportant. Edwards & Oakeshott (18) proposed a microcanonical ensemble for powders that maximized an entropy with volume as a conserved state variable, with the distinction from phase space that the states $\Omega(V)$ were restricted to jammed configurations (see **Figure 15**) (19). Recent experiments suggest that the zeroth law of thermodynamics does not hold for the resulting compactivity temperature. By incorporating force and torque balances, Henkes & Chakraborty (HC) (20) and Edwards & Blumenfeld (EB) (21, 22) derive a thermodynamics whereby a force-moment tensor $\hat{\Sigma}$ plays the role of energy and the intensive quantity $\hat{\alpha}$, named angoricity (stress in Greek), plays the role of temperature. The zeroth law so far appears to hold for angoricity.

lose heat as they nucleate, move, and tangle, and hence it would seem that no direct dislocation temperature should exist (25) distinct from the thermodynamic temperature. Many of these same concerns, however, apply to granular systems (26, 27), glassy simulations (28), and foams (29), all of which have shown evidence of effective temperatures and maximization of entropy (19). Dislocations also exchange force with the crystal lattice (pinned to inclusions, jogs, sessile dislocation junctions, etc.), presumably also arguing against a dislocation angoricity (see **Table 1** and sidebar titled Compactivity Versus Angoricity).

More prevalent in nonequilibrium statistical mechanics are studies of how particular rigid systems behave weirdly under forcing.[6] These other systems have attracted interest not because of the behavior as they are unloaded and reloaded, but rather because of the character of the microstates selected by the cycle of unloading and reloading. What can we glean from these systems about crystal plasticity?

The textbook picture of yield stress in crystals (11, 16) is particularly simple. Raising the stress to the yield stress and back to zero supposedly leaves the system in precisely the same state (ignoring creep); raising the stress beyond the yield stress leads to rearrangements of dislocations into new metastable configurations. Dislocations move and tangle under increasing stress, like snow gets pushed when a snowplow moves forward on the street. Under decreasing forcing, the dislocation tangles presumably remain in place just as the snow does.

Jog: the soliton mediating dislocation climb, left behind, e.g., when dislocations cross. Pins the dislocation

Magnets and other hysteretic systems have hysteresis upon decreasing and increasing the external field, but certain magnetic systems do return to precisely the same state upon reloading [the return-point memory effect (see **Figure 5*b***) and sidebar titled Magnetic Memory of Heating and

[6] A quantitative dislocation thermodynamics would seem incompatible with such weird behavior.

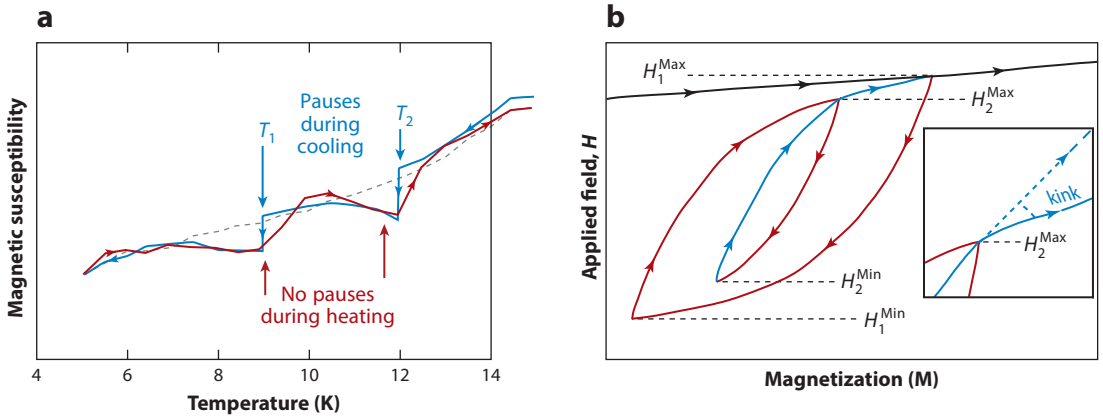

Figure 5

Disordered ferromagnets displaying return-point memory of the previous external field history.

MAGNETIC MEMORY OF HEATING AND BEATING

In **Figure 5*a***, spin glasses are frustrated magnetic systems, which have modes that are active in narrow ranges of temperatures. Annealing on cooling at temperatures T_1, T_2 leaves fewer susceptible modes upon heating through the same temperatures (30). In **Figure 5*b***, disordered ferromagnets at zero temperature have hysteresis loops that return to precisely the same microstates after the external field is decreased from $H^{\max 1}$ and returned to the previous maximum $H^{\max}$, even though the avalanches differ on raising and lowering the field. This is a return-point memory of the previous external field history (31). Each return to a previous maximum results in a kink in the $M(H)$ curve.

Beating)]. The avalanches these systems undergo upon unloading differ from those upon reloading. Upon increasing the external field H, $M(H)$ will have a kink at the point at which it rejoins the old trajectory. For a system trained into multiple hysteresis subloops, a kink arises upon raising the field above each (monotonically increasing) historical peak in the field history. In principle, a magnet could encode an indefinite number of such kinks, suggesting that no finite number of state variables can perfectly encode the behavior. Memory effects also arise from the thermal history in spin glasses, which encode pauses in the thermal history upon cooling (see **Figure 5*a*** and sidebar titled Magnetic Memory of Heating and Beating).

Another rigid state of matter is the charge density wave—a modulation in the electron density of a crystal whose wavelength can be unrelated (incommensurate) to the crystal lattice, and which is often pinned by impurities. The charge density wave in some materials can slide under a large enough external voltage. When slid repeatedly for a fixed pulse time t, the charge density wave settles into a stable limit cycle. Unlike the cases of return-point memory magnets and the simple model of plasticity, here the hysteretic behavior must be trained by a few cycles. These systems exhibit a striking collective effect, termed phase organization (32–34); the current at the end of the training pulse is always increasing, reflecting the marginal stability of the first periodic limit cycle found by local regions in the material. In the rough hypercube of possible periodic states, the ones selected are at hypercorners (see **Figure 6** and sidebar titled Phase Organization). This example warns us that the stuck states actually occupied in nonequilibrium systems can be distinct from typical metastable states in striking ways.

Kink: the soliton mediating dislocation glide across the Peierls barrier to the next lattice position. The barrier to kink motion is often tiny (10)

Peierls barrier: the barrier per unit length to dislocation glide due to the discreteness of the crystalline lattice; small for fcc metals

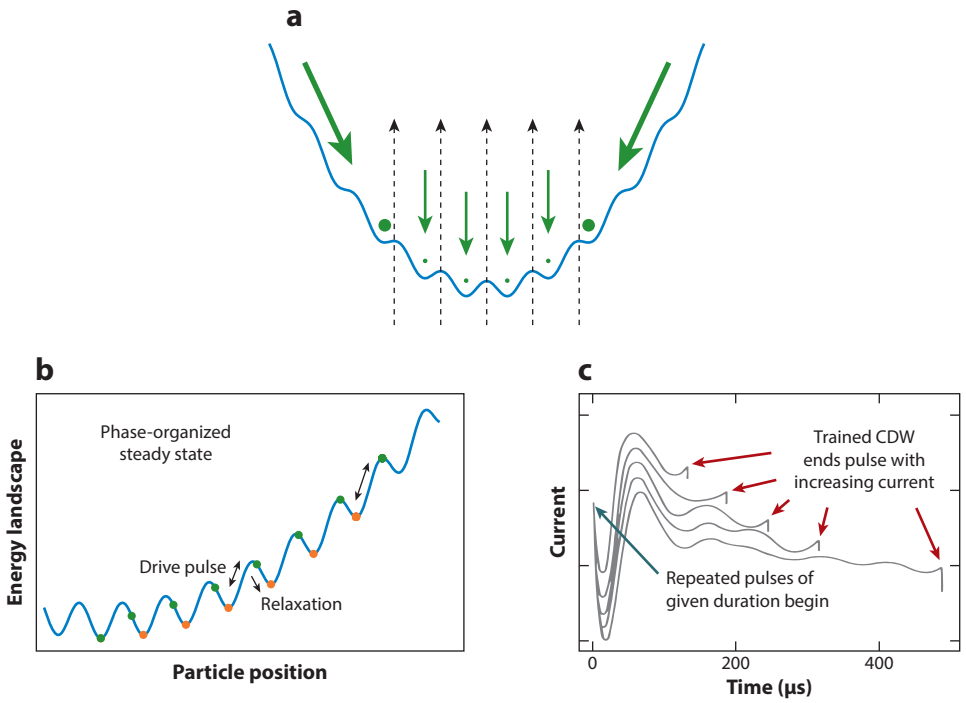

Figure 6

Nonequilibrium systems dynamically phase organize in a marginally stable configuration.

PHASE ORGANIZATION

Does a nonequilibrium system dynamically dumped into a stable state select typical or unusual metastable states? In **Figure 6*a***, consider a particle in a periodic potential, connected by a spring to a nail at the origin (32). A typical initial configuration will slide down the potential until the first local minimum, which will usually be on the edge of the range of local minima—just barely stable to inward forces. A collection of such nails (representing many local regions of a material), upon random initialization, will typically have most nails on their edges—a marginally stable hypercorner of the hypercube of possible system configurations. In **Figure 6*b***, for an ensemble of nailed particles trained by a pulse of a given duration (33), the pulses drive the particles up the spring potential, until realizing a phase-organized edge state in a marginally stable configuration at the end of the pulse. In **Figure 6*c***, in charge density wave (CDW) materials, this phenomenon leads to a current that always rises at the end of the pulse (33, 34).

We should note that the simple model of a yield stress, separating purely elastic behavior from irreversible deformation and determined purely from the previous stress maximum, is perhaps oversimplified; indeed, small amounts of hysteresis and training are probably to be expected in general. For example, if the stress swings negative, the dislocations will start to rearrange at absolute stresses somewhat lower than the yield stress [the Bauschinger effect (see Reference 16, chapter 6)]; reverse avalanches certainly happen as the stress direction is reversed. Because there are local stresses in a tangle due to the dislocation interactions that are comparable to the yield stress, it should be true that there are occasional backward avalanches on unloading: The local

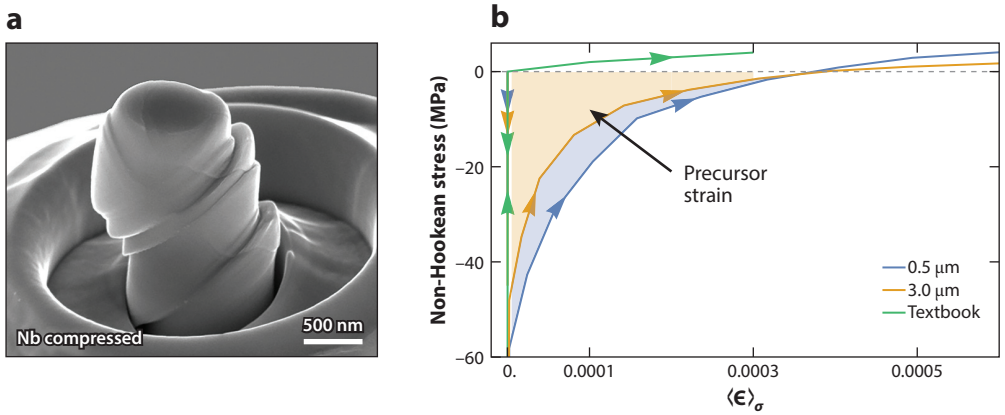

Figure 7

Compressed micropillars showing size-dependent precursor avalanche behavior.

AVALANCHE PRECURSORS

In **Figure 7*a***, micropillars under compression (when oriented properly) yield along a single glide plane. In **Figure 7*b***, dislocation avalanches become visible in these small-scale crystals. The macroscopic theory in textbooks (see Reference 35, chapter 26) predicts that under deformation the yield stress self-organizes to the current stress $\sigma_{\max}$ and that the material obeys Hooke's law as $\sigma_{ij} = C_{ijkl}\epsilon_{kl}$ upon unloading and reloading up to $\sigma_{\max}$. Here we show preliminary precision measurements by X. Ni & J.R. Greer (unpublished data) of the stress versus average strain upon reloading, for two different copper micropillars. The individual experiments clearly show precursor avalanches upon reloading, which are not a part of the macroscopic theory (36–38). These precursors average together into the stress-strain curves shown. The smaller net precursor strain occurs in the larger pillar; the precursor avalanches may entirely disappear in macroscopic samples.

material does not know when the point of zero external stress is crossed. Similarly, there will likely be some precursor avalanches upon reloading below the yield stress. Trained reversible states may have avalanches that differ upon loading and unloading but whose effects cancel. **Figure 7** and the sidebar titled Avalanche Precursors discuss preliminary results of micropillar compression experiments by X. Ni & J.R. Greer (unpublished data), with no avalanches upon unloading but precursor avalanches upon reloading before reaching the previous stress maximum. (Note that these precursor avalanches could be a finite-size effect, with smaller plastic strain for larger pillars.)

What do these examples suggest about state variables in theories of plastic flow in materials? It seems likely that crystalline dislocation networks do store their history in a way similar to that of spin glasses, magnets, and sliding charge density waves (see **Figure 5** and sidebar titled Magnetic Memory of Heating and Beating). One might naively predict that deforming a crystal in some pattern as it is cooled could, upon reheating, lead to a reversed echo deformation. In fact, bent crystals do not return to their original shapes when they are thermally annealed: A squashed nanopillar (see **Figure 7*a*** and sidebar titled Avalanche Precusors) does not stand up again upon heating. Instead, the deformation history after thermal annealing is reflected in surface steps (see **Figure 7*a*** and sidebar titled Avalanche Precursors) and (for polycrystals) in the grain orientation distribution [termed texture (41, 42)]. We must note, though, that shape-memory alloys do regain

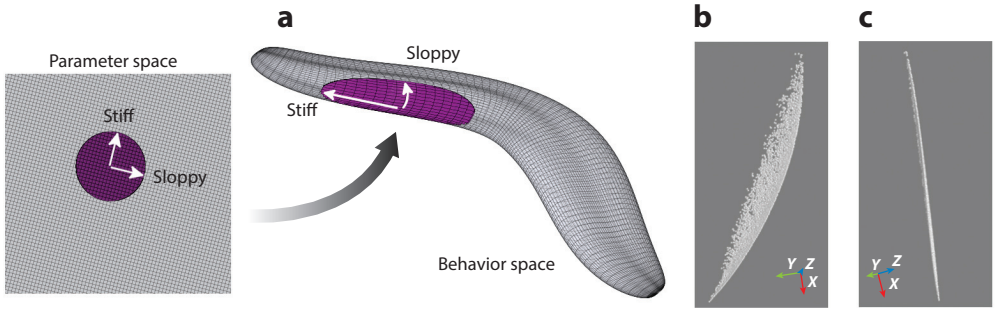

Figure 8

Manifolds and hyperribbon structure of a sloppy model. Panels *b* and *c* from Reference 40.

SLOPPY MODELS

Science is possible because of a kind of parameter compression (39). The behavior of complicated systems (cell biochemistry, interatomic potentials, insect flight, critical phenomena) can be expressed in a relatively simple way, controlled by a few stiff combinations of the microscopic parameters. Information geometry describes this phenomenon in terms of the manifold of all possible macroscale behaviors, which often forms a hyperribbon (40); sloppy parameter combinations move along the thin directions of this model manifold (see **Figure 8*a***). The model manifold for fitting curves to radioactive decay forms just such a hyperribbon (see **Figure 8*b*,*c***). Hence, it is challenging to extract lifetimes from a sum of exponential decays. Similar decay rates and amplitudes can be traded for one another along sloppy directions, with only stiff combinations constrained to keep the sum fixed. If we view the temperature and strain history in crystal plasticity as parameters and the macroscale anisotropic strength and toughness as behavior, this parameter compression could explain the emergence of effective plasticity theories with relatively few state variables encapsulating the stiff microscale combinations.

their original shapes upon reheating, due to the existence of a unique austenitic high-temperature state (43).

The fact that many historical parameters can be read from the current state does not preclude a useful low-dimensional description. Just because the current state of a material can encode its whole history does not mean that details of the history affect the behavior in significant ways. For example, although a magnet after ring-down (see **Figure 5** and sidebar titled Magnetic Memory of Heating and Beating) will show a cusp in the magnetization curve at every historical ring-down maximum, the cusps rapidly become tiny; the details of subloops of subloops of hysteresis loops are not crucial for understanding magnets. Indeed, this is a broad feature of nonlinear systems and models depending on many parameters; their behavior is usually well described by a few stiff combinations of parameters (see **Figure 8** and sidebar titled Sloppy Models). Perhaps yield stress, damage, porosity, and other local variables are capturing the stiff microscopic combinations governing macroscale behavior.

Finally, we must mention recent work on reversible-to-irreversible transitions (RITs) (see **Figure 9** and sidebar titled Hysteresis, Reversibility, and Irreversibility).[7] These are systems that

[7] Here we must distinguish local irreversibility from rearrangements such as avalanches, which do not reverse along the same path upon unloading, and global irreversibility, when the loading becomes large enough that cycling never settles down. The RIT in most cases is a transition from the former to the latter.

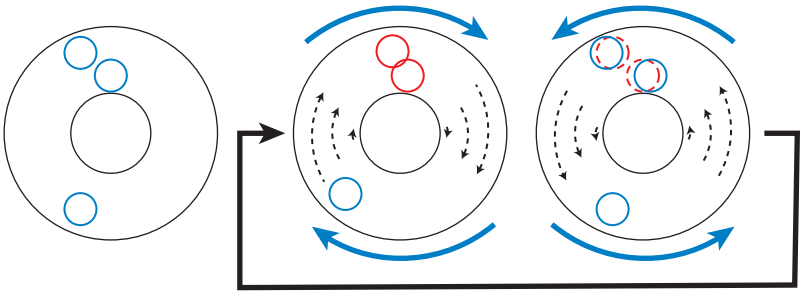

Figure 9

Illustration of reversible-to-irreversible transition for an experiment with colloids immersed in a forced viscous fluid.

HYSTERESIS, REVERSIBILITY, AND IRREVERSIBILITY

Forced viscous fluids (at low Reynold's numbers) reverse their motion when the forcing is reversed. When tiny colloidal particles are added, their trajectories reverse if they do not collide during the forward motion. Repeated oscillations at fixed amplitude can train the particles not to collide, mimicking crystals forced below their yield stress (44–50). Increasing the amplitude past the previous maximum training point yields new colloidal collisions. Similar transitions (except with hysteresis in the trained state) have been seen in amorphous solids (51–56), granular systems (57–60), dislocations (61), and superconducting vortices (62–68). If the density of colloidal particles is high or the shear amplitude is large, each collision can trigger on average one or more collisions in the next oscillation, leading to a reversible-to-irreversible transition, also observed in the other systems listed above; both the necessary cycling time and the length scales of the correlated rearrangements diverge with power laws, as discussed in Section 4.

can be trained into periodicity under low-amplitude cycles. In many systems, the number of cycles to train the system can grow to infinity at a critical amplitude, after which irreversible changes continue forever. This is our first example of a critical point exhibiting power laws and scaling functions—the topic of Section 4.

4. EMERGENT SCALE INVARIANCE IN PLASTICALLY DEFORMED CRYSTALS

When the external stress is raised above the yield stress, clear signs of collective behavior arise. Dislocations stretch, rearrange, and entangle to mediate plastic deformation, and their entanglement at least at first raises the yield stress (work hardening; see **Figure 3** and sidebar titled Dislocation Pinning and Word Hardening). Furthermore, there are two indications that the plastic deformation is associated with an emergent scale invariance (see **Figure 10** and sidebar titled Renormalization Group), with self-similar behavior on a broad range of length scales and timescales.

First, as in many rigid nonequilibrium systems, crystals respond to external stress via dislocation avalanches (see **Figure 11** and sidebar titled Avalanches). These avalanches have been observed in bulk ice crystal plasticity (79) and in micropillar plasticity of a variety of fcc and bcc metals (72, 80). Such avalanches come in a significant range of sizes, with a power-law probability distribution of the net slip $P(S) \sim S^{-\tau}$. The avalanches have a spatial fractal dimension d_f less than three (71, 81), mostly extending along slip bands. Such avalanches are seen in many other rigid statistical mechanical models under forcing (see **Figure 11** and sidebar titled Avalanches).

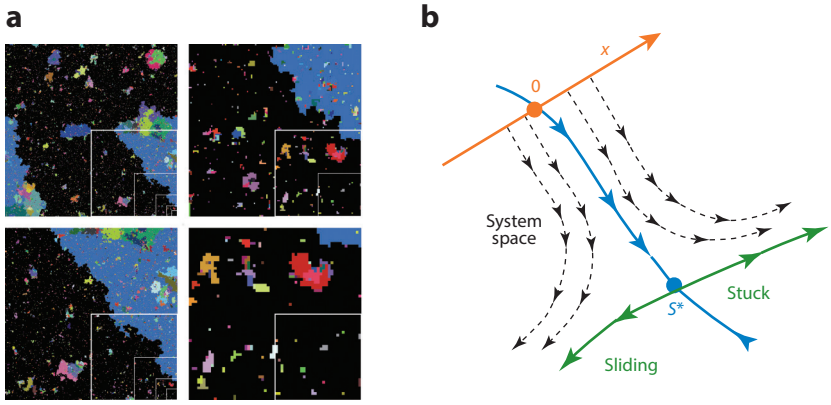

Figure 10

(*a*) Self-similarity and (*b*) renormalization group flow diagram.

RENORMALIZATION GROUP

The renormalization group (RG) (69) is an amazing abstraction that works in a system space, with dimensions parameterizing both different possible statistical models and real experiments. The RG studies how the rules governing a system change with length scale. By coarse graining (ignoring microscopic degrees of freedom up to a scale b), one derives rules with renormalized parameters—a dynamical flow in system space (*arrows* in **Figure 10*b***). In **Figure 10*a***, a RG fixed point S^* exhibits scale invariance, so, for example, the avalanches in space shows a statistical self-similarity upon zooming in to the lower right-hand corner (70). In **Figure 10*b***, tuning a parameter moves along a line (*red* in **Figure 10*b***) in system space; as the parameter flows across the stable manifold of S^* (*green* in **Figure 10*b***), the system will be self-similar after coarse graining to long length scales. Consider some observable Z (say, the avalanche size distribution) as a function of parameters x and y (which could be avalanche size, system size, stress, or the work-hardening coefficient). If Z, x, and y are eigenvectors of the linearized flow around S^*, then under coarse graining $Z(x, y) = b^{-\lambda_z} Z(xb^{\lambda_x}, yb^{\lambda_y})$, where λ is the corresponding eigenvalue. If we coarse grain until x flows to one (so $xb^{\lambda_x} = 1$), then

$$Z = x^{\frac{\lambda_z}{\lambda_x}} Z(1, yx^{-\frac{\lambda_y}{\lambda_x}}) = x^{\frac{\lambda_z}{\lambda_x}} \mathcal{Z}(yx^{-\frac{\lambda_y}{\lambda_x}}), \text{ or alternatively } Z = y^{\frac{\lambda_z}{\lambda_y}} \tilde{\mathcal{Z}}(yx^{-\frac{\lambda_y}{\lambda_x}}).$$

The observable is a power law times a universal scaling function $\tilde{\mathcal{Z}}$ of an invariant combination of parameters $yx^{-\lambda_y/\lambda_x}$. In plasticity, the probability $P \equiv Z$ of an avalanche of size $S \equiv y$ with a strain-hardening coefficient $\Theta \equiv x$ would be $P(S|\Theta) = S^{-\tau}\mathcal{P}(S/\Theta^{-d_f\nu})$, with $\mathcal{P} \equiv \tilde{\mathcal{Z}}$, $\tau \equiv -\lambda_z/\lambda_y$, and $\mathrm{d_f}\nu \equiv -\lambda_y/\lambda_x$.

This power-law distribution of slip sizes does not extend forever. Were the distribution a pure power law, the fraction of slip produced by avalanches larger than size S_0 would be $\int_{S_0}^{\infty} SP(S|L)\mathrm{d}S \propto S^{2-\tau}|_{S_0}^{\infty}$; because $1 < \tau < 2$, this would suggest that plastic deformation should be dominated by the largest events. The fact that the fractal dimension d_f of the avalanches is below three provides one natural cutoff. For a sample of size L, or a sample with avalanche-blocking internal structures, such as grain boundaries, of size L, the biggest avalanches will be of size L^{d_f}. Think of a simple model for micropillar deformation (see **Figure 7** and sidebar titled Avalanche Precursors), in which an avalanche induces one layer to slip over another over an area S along a slip direction. The largest avalanche will span the pillar, so $S \sim L^2$—but the pillar has changed

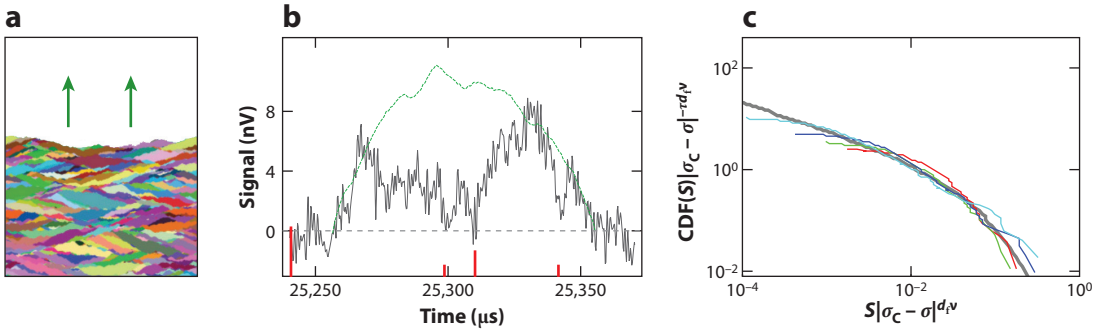

Figure 11

Avalanches in (*a*) depinning and (*b*) magnetic systems. (*c*) Scaling collapse of avalanche size distributions.

AVALANCHES

We define avalanches to be transitions from one metastable state to another under external forcing if these transitions span a broad range of sizes. They arise not only in plastic slip events (71, 72), but also in earthquakes (73, 74), fracture (75, 76), and many other systems (70). **Figure 11*a*** shows avalanches in a front depinning transition (77) (e.g., coffee invading a napkin dipped into the cup). **Figure 11*b*** shows a magnetic avalanche (78), illustrating the fractal structure in time t. The avalanche appears as a self-similar sequence of smaller events, each barely triggering the next (some large trigger events are marked by *red bars* in **Figure 11**), here a conjunction of two medium-sized avalanches, which are in turn conjunctions of small avalanches, etc. The green curve in **Figure 11** is the signal $\langle V(t)\rangle$ averaged over all avalanches of the same duration T; scaling (70) predicts $\langle V(t|T)\rangle \sim T^{1-d_f/z}\mathcal{V}(t/T)$, where z is a dynamic critical exponent. **Figure 11*c*** shows a scaling plot for the CDF (cumulative distribution function) of the dislocation avalanche sizes from micropillar experiments (72). The avalanche size cutoff grew with increasing stress (denoted by *different colors* in **Figure 11**), quantitatively following the mean-field prediction $P(S|\sigma) = S^{-\tau}\mathcal{P}(S/(\sigma_c - \sigma)^{-d_f\nu})$ (*gray curve* in **Figure 11**). Hence, avalanches can display scale invariance in time, space, and size.

height by only a few angstroms. More specifically (see **Figure 10** and sidebar titled Renormalization Group), the scaling distribution of avalanche sizes, cut off by a length L (system size, grain size, etc.), should take the form $P(S) \sim S^{-\tau}\mathcal{P}(S/L^{d_f})$. In many cases, it is believed (71) that the dominant cutoff in many cases is not due to the system size, but due to work hardening. As an avalanche proceeds, it increases the dislocation density in its immediate environment, raising the stress needed to produce further deformation. A work-hardening cutoff is also described by a scaling form $P(S) \sim S^{-\tau}\mathcal{P}(S/\Theta^{-d_f\nu})$, where $\Theta = \mathrm{d}\sigma_Y/\mathrm{d}\epsilon$ is the strain-hardening coefficient (the slope of the stress-strain curve due to work hardening).

The second indication of emergent scale invariance is the complexity of the dislocation tangles that emerge under plastic deformation. They are not homogeneous tangles of spaghetti—they develop correlated patterns with structure on many length scales. **Figure 12** and the sidebar titled Cell Structure and Scaling discuss a characteristic cell structure morphology found in deformed fcc metals. It is not yet clear whether cell structures are self-similar scale-invariant fractals (83, 85, 86) or whether they are similar to rescaled versions of the same system at different strains (84) (like coarsening; see **Figure 18** below). But the complex and yet patterned form of the tangles clearly indicates the need for a theory that embraces structures on different scales.

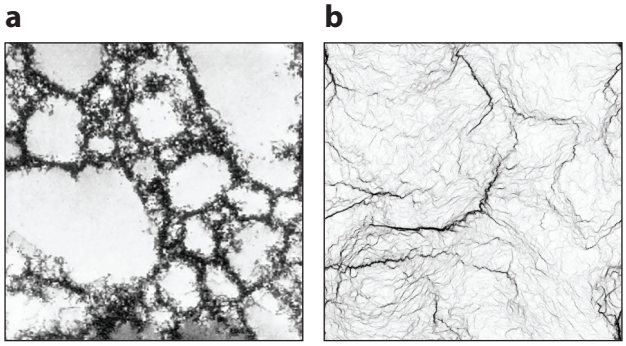

Figure 12

Dislocation wall structures from (*a*) TEM experiments [courtesy of Mughrabi (82) and Hähner et al. (83)] and (*b*) simulations.

CELL STRUCTURE AND SCALING

When dislocations interact, they do not just form a giant ball of spaghetti (smoothly varying distributions of highly entangled defects) but instead form interesting cell structures, with dislocation-poor cell interiors surrounded by dislocation-rich walls. Because these structures contain most of the defect content of the material, they dominate plastic deformation under load, with the walls providing a rigid backbone to the softer cell interiors (82). In **Figure 12*a***, just as the avalanches of dislocations (see **Figure 11** and sidebar titled Avalanches) occur on all timescales, these cell structures display structures on many length scales. Two different methods have been used to analyze cell structures. When analyzed using a single length scale, universal distributions emerge that are independent of material, loading process, or strain (84), refining with strain instead of coarsening with time (see **Figure 18** below). In an analysis using box counting of the dislocation density, others find that these cell structures exhibit fractal morphology (83). In **Figure 12*b***, continuum models, such as one such model by our group (85), are able to qualitatively reproduce the complex fractal cell morphologies of real materials by using grossly simplified models of dislocation dynamics. Our dislocation densities, misorientations, and other physical quantities can be described using power laws and scaling functions. We also reproduce the universal distributions and refinement observed by single-length scaling experimental analyses.

Systems with an emergent scale invariance—that look the same at different length scales and timescales—are a central focus of statistical physics. **Figure 10** and the sidebar Renormalization Group briefly summarize key ideas distilled from an enormous, sophisticated literature on a wide variety of systems. At a continuous transition between two qualitative behaviors (e.g., stuck to sliding as stress is tuned), many systems will exhibit scale-invariant fluctuations, with regions small and large alternating between the two qualitative behaviors. Renormalization group methods use this emergent self-similarity to predict power-law behavior of functions with one control parameter [like $P(S) \sim S^{-\tau}$ above] and to predict scaling forms for properties depending on more than one parameter [like $P(S|L) \sim S^{-\tau}\mathcal{P}(S/L^{d_f})$].

Our first example is drawn from another materials challenge, using scaling ideas to explain various aspects of fracture. First, much attention has been spent on fractal analyses of the resulting fracture surfaces (89–97). Two rival theories of crack growth in disordered materials (98–101) turned out to each describe the fractal height fluctuations observed in experiments (92, 93, 96, 102–108), one at short distances and one at longer distances. A crossover scaling theory (109, 110)

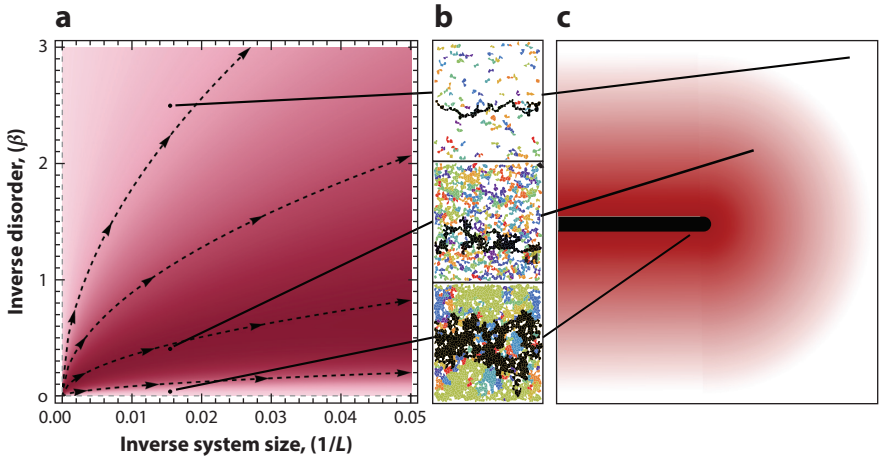

Figure 13

Quasi-brittle materials can display nucleated or uncorrelated fracture, depending on disorder—a scenario also applicable to damage around a growing crack.

FRACTURE IN DISORDERED MEDIA

Quasi-brittle materials like concrete are disordered, with a broad distribution of microscopic strengths (87) parameterized by inverse disorder β. **Figure 13*a*** shows a phase diagram of qualitative behavior, showing the crossover from nucleated (**Figure 13*a***, *upper left*) to percolative (**Figure 13*a***, *lower right*), through an intermediate range of avalanche-like precursors. In **Figure 13*b***, three simulations show qualitative behavior at different points in the phase diagram. **Figure 13*c*** shows the expected damage near a crack tip, with a corresponding crossover in behavior with distance. Low disorder or large sample size corresponds to brittle, nucleated fracture (**Figure 13*a***, *upper left*; **Figure 13*b***, *top*), whereas high disorder or small size corresponds to uncorrelated percolation-like fracture (**Figure 13*a***, *lower boundary*; **Figure 13*b***, *bottom*). The crossover between these regimes shows large avalanches (**Figure 13*b***, *middle*), whose mean second moment is indicated by red intensity. The renormalization group (RG) flows (**Figure 13*a***, *arrows*) predict that the distribution of avalanche sizes $P(s|\beta, L)$ has a crossover scaling form $P(s|\beta, L) = s^{-\tau}\mathcal{P}(\beta L^{1/\nu_f}, sL^{-1/\sigma\nu_f})$; no phase boundary separates the two regimes. **Figure 13*c*** shows that this scenario may also apply to the damage (schematically indicated by *red* intensity in **Figure 13*c***) in the region around a growing crack for an infinite system. Near the growing crack tip, stress is high and the material is reduced to rubble (percolation), whereas far from the crack tip, the stress is small and the material undamaged. The same RG crossover scaling analysis should allow us to develop a quantitative scaling theory of this damaged process zone (88).

produces a unified description of experimental height correlations on intermediate length scales. Second, in brittle materials, crack nucleation is studied with extreme value statistics (111–113)—the distribution of failure strengths is described by universal Gumbel and Weibull distributions, which have recently been viewed as renormalization group fixed points (114, 115).

The third scaling approach to fracture describes quasi-brittle materials like concrete, in which the strength of local regions is highly disordered (see **Figure 13** and sidebar titled Quasi-Brittle Materials). Similar to the case of dislocation avalanches in plastically deformed crystals, one observes a power-law distribution of microcrack avalanches preceding the eventual rupture (75, 76, 116–118). These are due to finite-size criticality (119): large avalanches in a crossover region

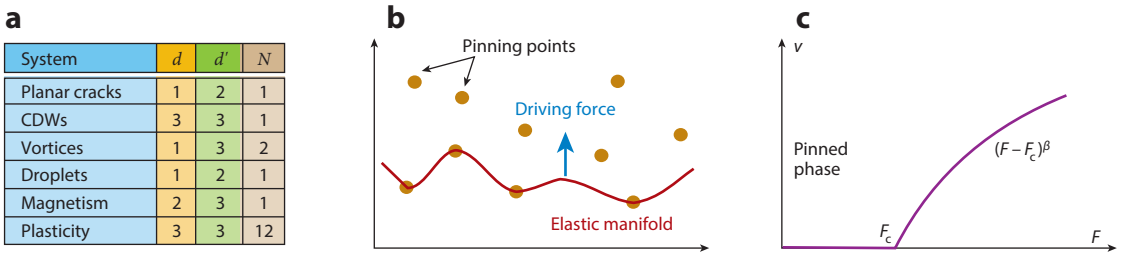

System	d	d'	N
Planar cracks	1	2	1
CDWs	3	3	1
Vortices	1	3	2
Droplets	1	2	1
Magnetism	2	3	1
Plasticity	3	3	12

Figure 14

Randomly pinned manifolds subject to an external force can exhibit depinning transitions and critical behavior.

DEPINNING AND CRITICALITY

In **Figure 14*a***, depinning transitions describe the jerky movement of surfaces pinned by disorder as they are dragged; they have been used to describe everything from planar cracks to superconducting vortices to raindrops on windshields (120). In **Figure 14*b***, a d-dimensional manifold is stuck on dirt in a d'-dimensional space and can move along N different directions. As the force increases, the system exhibits avalanche-like rearrangements of local regions, shifting between metastable states stuck in the dirt, until at a critical force the system starts sliding. In **Figure 14*c***, universal power laws and scaling behavior in the velocity and velocity autocorrelation above depinning and in the avalanche sizes, durations, shapes, and spatiotemporal correlations are explained using the emergent scale invariance at the depinning threshold. Fcc crystal plasticity is an example of a $d = d' = 3$ depinning transition, with $N = 12$ slip systems yielding under an external load [although $d = d' = 2$ and $N = 1$ in the simplest model (121, 122)]. Depinning transitions often have self-limiting terms that allow them to self-organize near critical points; work hardening plays this role for plasticity.

between two regimes, neither of which has bulk avalanches. At small sizes and large disorder, the bonds break in a percolation-like fashion (one at a time); at large sizes, a single dominant crack is nucleated in a rare event. Our finite-size scaling analysis should be generalizable to a crossover scaling theory for the process zone near the crack tip in quasi-brittle materials (see **Figure 13*c*** and sidebar titled Quasi-Brittle Materials). Combining these ideas with a scaling theory of plasticity (as described here) could allow for a crossover theory for the process zone for ductile fracture as well.

Two classes of models provide a particularly clear connection to the physics of plastically deformed crystals: the theory of depinning (described in **Figure 14** and sidebar titled Mesoscale Plasticity) and the theory of jamming (see **Figure 15** and sidebar titled Jamming). Both describe the response of a rigid system to external shear via avalanche-like rearrangements.

Process zone: the damaged zone near the tip of a crack, where linear elastic theory breaks down. For concrete, this zone can be nearly a meter in size

Depinning transitions describe motion in the presence of dirt, as for dislocations pinned primarily on second-phase precipitates. First, in fields like magnetic hysteresis and noise, depinning theories provide a comprehensive and compelling framework for understanding the experimental behavior (124) and are pursued using sophisticated functional renormalization group methods (125–129). Second, in fields like earthquakes, things are more controversial; the data do not discriminate so well between different models, but there is a broad consensus that scaling approaches are important and useful (130–132). Within the scaling theories, depinning models have had notable success (131, 133, 134) but remain in competition with other types of models (73, 135, 136). Part of the challenge is that the long-range interactions through the Earth's crust make

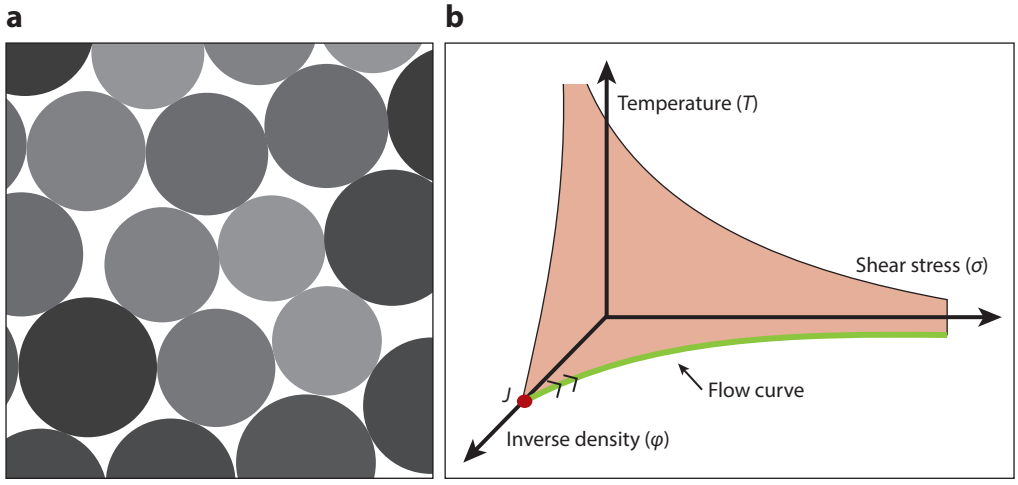

Figure 15

Illustrations of (*a*) a jammed packing and (*b*) a typical phase diagram of a jamming system.

JAMMING

Jamming (138, 139) attempts to describe the onset of rigidity in molecular glasses, granular media, colloids, pastes, emulsions, foams (139), dislocation systems (140), and biological tissues (141). At low temperature, low stress, and high density, the system is stuck in a jammed phase—a disordered solid state that resists shear. The jamming point J (see **Figure 15**) controls the critical behavior of the system. In contrast to depinning, in which dirt is explicitly part of the model, the disorder in a jammed system is frozen in as it jams—just as dislocations in crystals tangle themselves up as they evolve (140, 142, 143). At point J, one finds the power laws, scaling collapses, and diverging length scales (138, 139) that are characteristic of systems with emergent scale invariance (see **Figure 10** and sidebar titled Renormalization Group), although no coarse-graining approach has yet been developed. A recent scaling ansatz (144) argues that the free energy has the scaling form $F(\Delta\varphi, P, \sigma, T) = \Delta\varphi^2 \mathcal{F}_0(P/\Delta\varphi, \sigma/\Delta\varphi^{5/4}, T/\Delta\varphi^2)$, where (as usual) the arguments of the scaling function are invariant under the presumed renormalization group flow (see **Figure 10** and sidebar titled Renormalization Group), with mean-field rational critical exponents in three dimensions. In particular, a point near J along the zero-temperature yielding boundary (the *green curve* in the φ-σ plane), when coarse grained, must also be a system at its yield point, farther from point J. This implies that the combination $\sigma/\Delta\varphi^{5/4}$ is invariant along the yielding curve, so $\sigma_{\text{flow}} \propto \Delta\varphi^{5/4}$ (145–147). Jammed states may develop equilibrium-like properties; they seem to maximize entropy [become equally probable (19)] and to have thermodynamic descriptions (see References 26–29 and **Table 1**). Perhaps the weird memory effects of Section 3 are erased by the large fluctuations near critical points.

the theory mean field (137), allowing many different microscopic theories to yield the same behavior. Finally, many of the statistical theories of plasticity in crystals are depinning theories (see **Figure 16** and sidebar titled Mesoscale Plasticity).

Jamming transitions (138, 139) describe the elastic response of systems near the point at which the constituent particles first assemble into a rigid network. The hardness of clean single crystals is primarily due to dislocation entanglement with other dislocations—the disordered pinning is

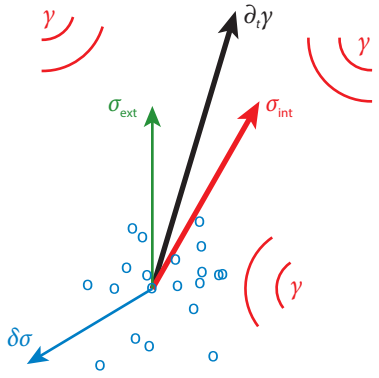

Figure 16

Caricature of the different terms appearing in a typical mesoscale plasticity depinning model.

MESOSCALE PLASTICITY

$$\frac{1}{B}\partial_t\gamma(\boldsymbol{r}) = \sigma_{\text{ext}} + \sigma_{\text{int}}(\boldsymbol{r}) + \delta\sigma(\boldsymbol{r},\gamma),$$

$$\sigma_{\text{int}}(\boldsymbol{k}) = -\frac{G}{\pi(1-\nu)\gamma(\boldsymbol{k})}\frac{k_x^2 k_y^2}{|\boldsymbol{k}|^4}. \qquad 1.$$

The above mesoscale plasticity evolution equation (from Reference 121) is typical of depinning: The evolution of the manifold γ depends on an external driving force σ_{ext}, a nonlocal force σ_{int} due to the rest of the manifold, and a force $\delta\sigma(\boldsymbol{r},\gamma)$ due to dirt and other dislocations at $\boldsymbol{r}$ (see **Figure 16**). Here γ is the shear strain (up to 12 components), G the shear modulus, ν the Poisson ratio, and B a viscoplastic rate coefficient. The nonlocal kernel given in Fourier space by the second equation shown above is characteristic of all elastic materials—both crystalline and amorphous (122, 123). Plasticity is different from most depinning problems for two reasons. First, the kernel is not convex (positive and negative in different directions), making most of the analytic methods challenging. Second, dislocations tangle among themselves even without dirt. Like glasses and jammed systems, such dislocations generate their own disorder as they evolve.

Recrystallization: an abrupt change in the morphology of a work-hardened crystal, whereby the dislocations become so dense that they spontaneously annihilate, mediated by a large-angle grain boundary that sweeps through the system

not static but dynamically evolves as the dislocations jam together, making the analogy with the jamming critical point perhaps more plausible (140, 142, 143).

In plastically deformed crystals, what is the critical point? What corresponds to the depinning force in **Figure 14** or point J in **Figure 15**? Let us consider a system in which the slope of the work-hardening curve $\Theta = \mathrm{d}\sigma_Y/\mathrm{d}\epsilon$ controls the cutoff in the avalanche size distribution and presumably also the cutoff for the fractal self-similarity in the spatial morphology. The critical point $\Theta = 0$ (which flows to a self-similar fixed point under the renormalization group in **Figure 10**) corresponds to a material that does not work harden with increasing strain.

Such a material would either continue to deform at constant stress [perhaps related to superplasticity (148)] or begin to weaken with further stress [as happens in metallic glasses, leading to shear band failure (14, 15)]. Evidence for a plain old (as opposed to self-organized) critical point at a stress σ_c has been seen in micropillar experiments (72) (see **Figure 11*c***) and sidebar titled Avalanches), in which the avalanche sizes diverge at a σ_c that we term the critical failure stress.

Such experiments find quantitative agreement with a mean-field scaling theory, for a traditional critical point, with a scaling form for the avalanche sizes $P(S|\sigma) \sim S^{-\tau}\mathcal{P}[S/(\sigma_c - \sigma)^{-d_f\nu}]$.

Much of the statistical physics literature describes crystal plasticity instead as a self-organized critical point (157). Depinning systems like earthquakes are thought to exhibit emergent scale invariance without fine-tuning to a critical point because the natural microscopic velocities (tectonic plates drift centimeters/year) are tiny compared to the mean velocities during avalanches (70). In many macroscopic materials, work hardening under increasing stress or strain does not peak at a critical stress or strain. Instead, it terminates in a qualitative way—fracture (breaking in two), amorphization (in which the crystalline correlations drop to the atomic scale), or perhaps recrystallization (158). Also, the natural scale of the work-hardening coefficient Θ is comparable to the elastic modulus; one prediction (71) for the cutoff of the avalanche size distribution is a slip[8] of $S_0 = L^2E/\Theta$—small compared to macroscopic scales but large compared to atomic scales for large system size L. Thus, the natural cutoff scale due to work hardening for macroscopic samples is tiny, just as the velocities of earthquake fronts are tiny, leading to a self-organized critical point.[9]

A key test for scaling theories of plasticity is the exponent τ giving the power law for the avalanche size distribution. Many experiments on crystalline and amorphous plasticity can be fit using a value $\tau \sim 3/2$ (151). Whereas older simulations seemed to agree with this value (159, 160), newer simulations observe smaller values of $\tau \sim 1.25–1.4$ (14, 154–156, 161).[10]

It is not clear at this time what governs these variations, but one intriguing hint is provided by two different mean-field theories for plasticity (see **Figure 17** and sidebar titled Mean-Field Theory and Plasticity). A local rearrangement of atoms at a site will yield a net plastic slip, producing a long-range, anisotropic change in the stress. This elastic dipole adds to the imposed stress in some directions and relieves the stress in others, often triggering disconnected pieces of the avalanche elsewhere in the system. Some mean-field theories (122, 151) have ignored the variation in sign of this interaction; the argument is that the directional anisotropy makes the positive interactions within a slip band or glide plane the only important ones (133). This leads to a theory in which every site feels a monotonically increasing external stress, which in mean field gives the exponent $\tau = 3/2$. Others (150, 164) have ignored the directional anisotropy and argue that the random positive and negative changes in stress lead to a kind of anomalous diffusion in the distance of each site from its local yielding stress. Any site that crosses its yielding stress triggers an avalanche and disappears from the active list, carving a hole out of the distribution of sites near their critical stress. This hole leads to fewer, larger avalanches and a lower value for τ.

We end with a cautionary note particularly addressed to the statistical physics community. Emergent scale invariance in physics leads not only to power laws and scaling functions but also to universality—any two critical systems that flow to the same fixed point in **Figure 10** will share the same long-wavelength behavior. Thus, the Ising model quantitatively describes both (*i*) the disappearance of magnetism with increasing temperature in some magnets and (*ii*) the disappearance of the density difference between liquid and vapor along the coexistence line as temperature and

[8]We define S to be the net slip. Csikor et al. (71) define the avalanche size s to be the strain jump, which is bS/L^3, because a slip of size L^2 causes the material to shrink by approximately a Burgers vector $\delta L/L \sim b/L$. The cutoff used by Csikor et al. is at constant load $s_0 = bE/L\Theta$, which thus becomes a cutoff in our notation of $S_0 = L^2E/\Theta$.

[9]Here there are two different relevant variables at the fixed point, $1/L$ and Θ. The predicted scaling form for the avalanche size distribution $P(S|\Theta, L) \sim S^{-\tau}\mathcal{P}(S/L^{d_f}, L/\Theta^{-\nu})$ gives the distribution used by Csikor et al. (71) $P(S) = S^{-\tau}e^{(S/S_0)^2}$ if we assume $\mathcal{P}(X, Y) = \exp\left[(XY^{1/\nu})^2\right]$ and $d_f - 1/\nu = 2$. Note that this makes sense only if $d_f > 2$, different from that proposed by Csikor et al. but compatible with $d_f \sim 2.5$ found by Weiss & Marsan (81).

[10]One set of experiments (162) showed a rate dependence yielding values of $\tau > 1.5$ for slow deformations; these experiments have been modeled as a quasi-periodic approach to a critical point punctuated by quasi-periodic system-spanning events (163).

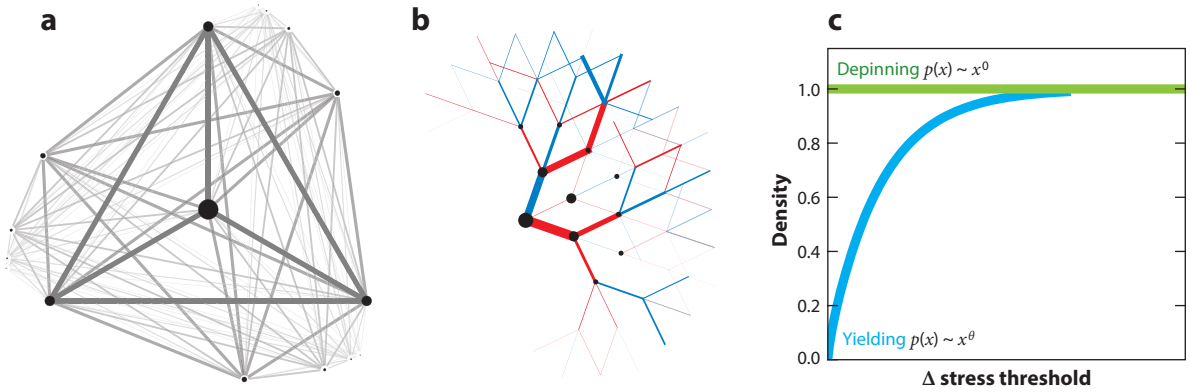

Figure 17

Fully connected (*a*) or Cayley-tree (*b*) mean-field theories provide a useful description of the yielding transition in plasticity (*c*).

MEAN-FIELD THEORY AND PLASTICITY

Figure 17*a*,*b* shows mean-field theories describe systems in high dimensions or with long-range forces. Some theories assume that each degree of freedom feels the mean of other sites as in a fully connected hypertetrahedron (**Figure 17*a***); others sit on an infinite branching tree (Bethe lattice; **Figure 17*b***). With a plastic rearrangement, the anisotropic stress increases the loading on some neighbors and decreases it on others. Some authors focus on the decrease but ignore the anisotropy (149, 150); other authors argue that the anisotropy allows one to ignore the decrease (122, 151). In **Figure 17*c***, for systems of the former type, the density of sites close to their failure threshold must be suppressed due to past fluctuations crossing the threshold, forming a pseudogap scaling as $(\sigma_c - \sigma)^\theta$. This yields a value of $\tau \leq 3/2$ that depends on the long-range tail in the coupling distribution. For the latter, no pseudogap appears, and the distribution of avalanche sizes scales as $P(S) \sim S^{-\tau}$, where $\tau = 3/2$. A wide variety of experiments are consistent with $\tau = 3/2$ (78, 79, 152, 153). In contrast, some simulations suggest that $\tau \approx 1.3$ (154–156).

pressure are increased. In contrast, success in materials physics has historically rested upon attention to materials-specific details. Many metallurgists focus their careers on specific materials. Aluminum alloys, steels, and titanium superalloys are worlds unto themselves. Are the scaling methods of statistical physics doomed in the attempt to describe the bewildering variety of anisotropic slip systems, dislocation mobilities, cross slip, pinning, and so forth?

Here we remind our statistical colleagues of a simple but profound observation by Rutenberg & Vollmayr-Lee (165) some decades ago (see **Figure 18** and sidebar titled Nonuniversality): Our scaling theory of coarsening is an example in which the universality class is parameterized by entire anisotropic functions of angle. There is no good reason why this kind of strong materials dependence should be incompatible with scaling and criticality. Also, there will likely be several universality classes, depending upon the active mechanisms for plastic deformation; systems with one active slip system behave very differently from the same material at later stages, at which multiple systems and cross slip become active. Our attempts to form a scaling theory must focus not only on what makes plastic deformation the same among materials composition and processing history, but also on what makes each system different.

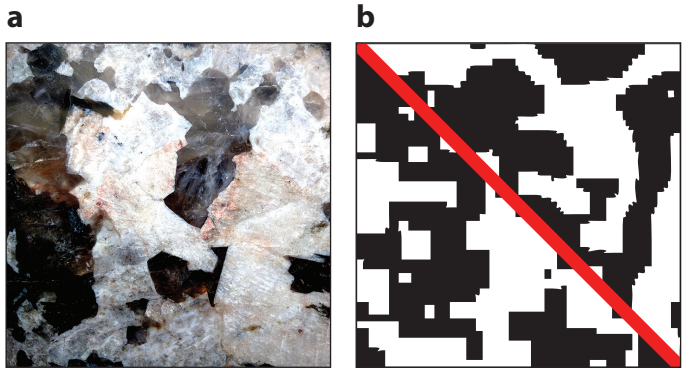

Figure 18

Polycrystalline granite (*a*) and coarsened configurations of the 3D Ising model (*b*), with (*lower*) and without (*upper*) the addition of next-neighbor antiferromagnetic interactions. Which side of panel *b* resembles granite?

NONUNIVERSALITY

Figure 18*a* shows polycrystalline granite. When magma slowly cools below the Earth's surface, it coarsens into different component crystals, forming granite. Scaling theories that describe coarsening have inverse time as a relevant variable. When $r \to r/b$, the time rescales as $t \to t/b^3$ (see **Figure 10** and sidebar titled Renormalization Group; see also Reference 7, section 11.4.1). Thus, both salad dressing and the Ising model near T_c are described by the same correlation function $C(\mathbf{r}, t) = \mathcal{C}(r/t^{1/3})$ because coarsening in isotropic systems is universal. In 1999, Rutenberg & Vollmayr-Lee (165) noted that this is not true of anisotropic crystalline systems or of the Ising model away from T_c; although a scaling form exists, it is dependent on the anisotropic surface tensions and interface mobilities. **Figure 18*b*** compares coarsening in the 3D Ising model (*upper triangle* in **Figure 18*b***) with the same system with additional weak antiferromagnetic next-neighbor bonds (*lower triangle* in **Figure 18*b***). The added interaction slows coarsening to $r \sim \log(t)$ and introduces a preference for flat boundaries aligned with the lattice directions (166), producing facets like those in granite (**Figure 18*a***). Although physicists are fond of universality, the world is filled with a bewildering variety of rocks and dislocation tangles. Many materials-dependent properties must likely be treated as relevant variables in our eventual scaling theory of plasticity, as they are for coarsening.

SUMMARY POINTS

1. Crystals are a challenge for nonequilibrium statistical mechanics. Our methods addressing disorder, long-range forces, constrained dynamics, and anisotropic interactions must be combined to address dislocation entanglement in crystal plasticity.
2. There are many rigid statistical mechanical systems with behavior closely analogous to the yield stress and work hardening seen in crystal plasticity. Upon unloading, these simpler systems are left in configurations that are rare among the possible metastable states, encoding the materials history in interesting ways.
3. The thermal and mechanical history of a crystal is thus probably encoded in its morphology. This need not prevent a phenomenological theory from effectively encapsulating its future macroscale behavior.

4. Avalanche dynamics and the morphologies of dislocation tangles provide clear evidence that plastically deformed crystals exhibit an emergent scale invariance.
5. Strong analogies can be made between the avalanches observed in plasticity and the scaling behavior seen in fracture, depinning, jamming, and even dilute colloidal suspensions under shear.
6. Crystal plasticity is immensely complex and strongly material and history dependent. A successful renormalization group scaling theory of plasticity in crystals will depend on far more details about the microscopic behavior than has been typical in previous systems exhibiting scale invariance.

DISCLOSURE STATEMENT

The authors are not aware of any affiliations, memberships, funding, or financial holdings that might be perceived as affecting the objectivity of this review.

ACKNOWLEDGMENTS

We thank Bulbul Chakraborty, Karen Daniels, Andrea J. Liu, and M. Lisa Manning for extensive consultation. We also thank Paul Dawson, Ryan Elliott, Susan Coppersmith, James Jenkins, and Ellad Tadmor for kindly providing references and/or permission to reprint figures. J.P.S., M.K.B., D.B.L., and A.R. were supported by the Department of Energy through grant DE-FG02-07ER46393. L.X.H., J.P.K.-D., E.D.L., and K.N.Q. were supported by the National Science Foundation (NSF) through grant NSF DMR-1312160. K.A.D. is thankful for support from the NSF through grant CBET 1336634 and also thanks the Kavli Institute of Theoretical Physics for hospitality and support through NSF grant PHY11-25915. C.P.G. is supported by the NSF through the Harvard Materials Research Science and Engineering Center (DMR1420570) and the Division of Mathematical Sciences (DMS-1411694). J.R.G. and X.N. are grateful to the US Department of Energy (DOE) through J.R.G.'s Early Career Research Program under grant DE-SC0006599. L.X.H. was supported by a fellowship from Cornell University. E.D.L. acknowledges support by the NSF through the GRFP fellowship (DGE-1650441). K.N.Q. was supported by the Natural Sciences and Engineering Research Council of Canada. D.Z.R. acknowledges support through the Bethe/KIC Fellowship and NSF grant DMR-1308089. A.S. acknowledges support from the Miller Fellowship by the Miller Institute for Basic Research in Science at the University of California, Berkeley. S.Z. is supported by the European Research Council advanced grant SIZEFFECTS.

LITERATURE CITED

1. Chandler D. 1987. *Introduction to Modern Statistical Mechanics*. Oxford, UK: Oxford Univ. Press
2. Forster D. 1995. *Hydrodynamic Fluctuations, Broken Symmetry, and Correlation Functions*. Reading, MA: Perseus Books
3. Martin PC. 1968. *Problème à n corps (Many Body Physics)*. New York: Gordon and Breach
4. Landau L, Lifshitz E. 2013. *Statistical Physics*. Vol. 5. Oxford, UK: Elsevier Sci.
5. Tadmor EB, Miller RE, Elliott RS. 2012. *Continuum Mechanics and Thermodynamics: From Fundamental Concepts to Governing Equations*. Cambridge, UK: Cambridge Univ. Press
6. Anderson PW. 1978. Lectures on amorphous systems. In *Les Houches Session XXXI*, ed. R Balian, R Maynard, G Toulouse, pp. 158–261. Singapore: World Sci.

7. Sethna JP. 2006. *Statistical Mechanics: Entropy, Order Parameters, and Complexity*. **http://www.physics.cornell.edu/sethna/StatMech/**. Oxford, UK: Oxford Univ. Press
8. Chui ST, Weeks JD. 1978. Dynamics of the roughening transition. *Phys. Rev. Lett.* 40:733–36
9. Liarte DB, Bierbaum M, Mosna RA, Kamien RD, Sethna JP. 2016. Weirdest martensite: smectic liquid crystal microstructure and Weyl-Poincaré invariance. *Phys. Rev. Lett.* 116:147802
10. Vegge T, Sethna JP, Cheong SA, Jacobsen KW, Myers CR, Ralph DC. 2001. Calculation of quantum tunneling for a spatially extended defect: The dislocation kink in copper has a low effective mass. *Phys. Rev. Lett.* 86:1546–49
11. Hull D, Bacon DJ. 2011. *Introduction to Dislocations*. Vol. 37. Oxford, UK: Elsevier
12. Bulatov VV, Hsiung LL, Tang M, Arsenlis A, Bartelt MC, et al. 2006. Dislocation multi-junctions and strain hardening. *Nature* 440:1174–78
13. Taylor GI. 1934. The mechanism of plastic deformation of crystals. I. Theoretical. *Proc. R. Soc. Ser. A Math. Phys. Eng. Sci.* 145:362–87
14. Budrikis Z, Zapperi S. 2013. Avalanche localization and crossover scaling in amorphous plasticity. *Phys. Rev. E* 88:062403
15. Sandfeld S, Budrikis Z, Zapperi S, Castellanos DF. 2015. Avalanches, loading and finite size effects in 2D amorphous plasticity: results from a finite element model. *J. Stat. Mech. Theory Exp.* 2015:P02011
16. Dieter GE, Bacon DJ. 1986. *Mechanical Metallurgy*. Vol. 3. New York: McGraw-Hill
17. Bi D, Henkes S, Daniels KE, Chakraborty B. 2015. The statistical physics of athermal materials. *Annu. Rev. Condens. Matter Phys.* 6:63–83
18. Edwards S, Oakeshott R. 1989. Theory of powders. *Physica A Stat. Mech. Appl.* 157:1080–90
19. Martiniani S, Schrenk KJ, Ramola K, Chakraborty B, Frenkel D. 2016. Are some packings more equal than others? A direct test of the Edwards conjecture. arXiv:1610.06328 [cond-mat.soft]
20. Henkes S, Chakraborty B. 2005. Jamming as a critical phenomenon: a field theory of zero-temperature grain packings. *Phys. Rev. Lett.* 95:198002
21. Edwards S. 2005. The full canonical ensemble of a granular system. *Physica A Stat. Mech. Appl.* 353:114–18
22. Blumenfeld R, Edwards S. 2009. On granular stress statistics: compactivity, angoricity, and some open issues. *J. Phys. Chem. B* 113:3981–87
23. Jenkins JT. 2015. Kinetic theories for collisional grain flows. In *Handbook of Granular Materials*, ed. SV Franklin, MD Shattuck, pp. 155–86. Boca Raton, FL: CRC Press
24. Puckett JG, Daniels KE. 2013. Equilibrating temperaturelike variables in jammed granular subsystems. *Phys. Rev. Lett.* 110:058001
25. Langer J, Bouchbinder E, Lookman T. 2010. Thermodynamic theory of dislocation-mediated plasticity. *Acta Mater.* 58:3718–32
26. Makse HA, Kurchan J. 2002. Testing the thermodynamic approach to granular matter with a numerical model of a decisive experiment. *Nature* 415:614–17
27. Abate AR, Durian DJ. 2008. Effective temperatures and activated dynamics for a two-dimensional air-driven granular system on two approaches to jamming. *Phys. Rev. Lett.* 101:245701
28. Berthier L, Barrat JL. 2002. Shearing a glassy material: numerical tests of nonequilibrium mode-coupling approaches and experimental proposals. *Phys. Rev. Lett.* 89:095702
29. Ono IK, O'Hern CS, Durian DJ, Langer SA, Liu AJ, Nagel SR. 2002. Effective temperatures of a driven system near jamming. *Phys. Rev. Lett.* 89:095703
30. Jonason K, Vincent E, Hammann J, Bouchaud J, Nordblad P. 1998. Memory and chaos effects in spin glasses. *Phys. Rev. Lett.* 81:3243
31. Sethna JP, Dahmen K, Kartha S, Krumhansl JA, Roberts BW, Shore JD. 1993. Hysteresis and hierarchies—dynamics of disorder-driven first-order phase transformations. *Phys. Rev. Lett.* 70:3347–50
32. Coppersmith S. 1987. A simple illustration of phase organization. *Phys. Lett. A* 125:473–75
33. Coppersmith S, Littlewood P. 1987. Pulse-duration memory effect and deformable charge-density waves. *Phys. Rev. B* 36:311
34. Tang C, Wiesenfeld K, Bak P, Coppersmith S, Littlewood P. 1987. Phase organization. *Phys. Rev. Lett.* 58:1161

35. Asaro R, Lubarda V. 2006. *Mechanics of Solids and Materials*. Cambridge, UK: Cambridge Univ. Press
36. de Silva CW. 2013. *Mechanics of Materials*. Boca Raton, FL: CRC Press
37. Nair S. 2015. *Mechanics of Aero-Structures*. Cambridge, UK: Cambridge Univ. Press
38. Philpot T. 2012. *Mechanics of Materials: An Integrated Learning System*. Hoboken, NJ: Wiley Glob. Educ. 3rd ed.
39. Machta BB, Chachra R, Transtrum M, Sethna JP. 2013. Parameter space compression underlies emergent theories and predictive models. *Science* 342:604–7
40. Transtrum MK, Machta BB, Brown KS, Daniels BC, Myers CR, Sethna JP. 2015. Perspective: Sloppiness and emergent theories in physics, biology, and beyond. *J. Chem. Phys.* 143:010901
41. Kocks UF, Tomé CN, Wenk HR. 2000. *Texture and Anisotropy: Preferred Orientations in Polycrystals and Their Effect on Materials Properties*. Cambridge, UK: Cambridge Univ. Press
42. Randle V, Engler O. 2000. *Introduction to Texture Analysis: Macrotexture, Microtexture and Orientation Mapping*. London: Gordon and Breach
43. Bhattacharya K. 2003. *Microstructure of Martensite: Why It Forms and How It Gives Rise to the Shape-Memory Effect*. Oxford, UK: Oxford Univ. Press
44. Corté L, Chaikin PM, Gollub JP, Pine DJ. 2008. Random organization in periodically driven systems. *Nat. Phys.* 4:420–24
45. Pine D, Gollub J, Brady J, Leshansky A. 2005. Chaos and threshold for irreversibility in sheared suspensions. *Nature* 438:997–1000
46. Paulsen JD, Keim NC, Nagel SR. 2014. Multiple transient memories in experiments on sheared non-Brownian suspensions. *Phys. Rev. Lett.* 113:068301
47. Reichhardt C, Reichhardt CJO. 2009. Random organization and plastic depinning. *Phys. Rev. Lett.* 103:168301
48. Keim NC, Arratia PE. 2013. Yielding and microstructure in a 2D jammed material under shear deformation. *Soft Matter* 9:6222–25
49. Keim NC, Arratia PE. 2014. Mechanical and microscopic properties of the reversible plastic regime in a 2D jammed material. *Phys. Rev. Lett.* 112:028302
50. Menon GI, Ramaswamy S. 2009. Universality class of the reversible-irreversible transition in sheared suspensions. *Phys. Rev. E* 79:061108
51. Regev I, Weber J, Reichhardt C, Dahmen KA, Lookman T. 2015. Reversibility and criticality in amorphous solids. *Nat. Commun.* 6:8805
52. Regev I, Lookman T, Reichhardt C. 2013. Onset of irreversibility and chaos in amorphous solids under periodic shear. *Phys. Rev. E* 88:062401
53. Fiocco D, Foffi G, Sastry S. 2013. Oscillatory athermal quasistatic deformation of a model glass. *Phys. Rev. E* 88:020301(R)
54. Jeanneret R, Bartolo D. 2014. Geometrically protected reversibility in hydrodynamic Loschmidt-echo experiments. *Nat. Commun.* 5:3474
55. Nagamanasa KH, Gokhale S, Sood AK, Ganapathy R. 2014. Experimental signatures of a nonequilibrium phase transition governing the yielding of a soft glass. *Phys. Rev. E* 89:062308
56. Rogers MC, Chen K, Andrzejewski L, Narayanan S, Ramakrishnan S, et al. 2014. Echoes in X-ray speckles track nanometer-scale plastic events in colloidal gels under shear. *Phys. Rev. E* 90:062310
57. Möbius R, Heussinger C. 2014. (Ir)reversibility in dense granular systems driven by oscillating forces. *Soft Matter* 10:4806–12
58. Schreck CF, Hoy RS, Shattuck MD, O'Hern CS. 2013. Particle-scale reversibility in athermal particulate media below jamming. *Phys. Rev. E* 88:052205
59. Slotterback S. 2012. Onset of irreversibility in cyclic shear of granular packings. *Phys. Rev. E* 85:021309
60. Royer JR, Chaikin PM. 2015. Precisely cyclic sand: self-organization of periodically sheared frictional grains. *PNAS* 112:49–53
61. Zhou C, Olson Reichhardt C, Reichhardt C, Beyerlein I. 2014. Random organization in periodically driven gliding dislocations. *Phys. Lett. A* 378:1675
62. Okuma S, Tsugawa Y, Motohashi A. 2011. Transition from reversible to irreversible flow: absorbing and depinning transitions in a sheared-vortex system. *Phys. Rev. B* 83:012503

63. Mangan N, Reichhardt C, Reichhardt C. 2008. Reversible to irreversible flow transition in periodically driven vortices. *Phys. Rev. Lett.* 100:187002
64. Pérez Daroca D, Pasquini G, Lozano GS, Bekeris V. 2011. Dynamics of superconducting vortices driven by oscillatory forces in the plastic-flow regime. *Phys. Rev. B* 84:012508
65. López D, Kwok WK, Safar H, Olsson RJ, Petrean AM, et al. 1999. Spatially resolved dynamic correlation in the vortex state of high temperature superconductors. *Phys. Rev. Lett.* 82:1277–80
66. Miguel MC, Zapperi S. 2003. Tearing transition and plastic flow in superconducting thin films. *Nat. Mater.* 2:477
67. Shaw G, Mandal P, Banerjee SS, Niazi A, Rastogi AK, et al. 2012. Critical behavior at depinning of driven disordered vortex matter in 2H-NbS_2. *Phys. Rev. B* 85:174517
68. Okuma S, Motohashi A. 2012. Critical behavior associated with transient dynamics near the depinning transition. *New J. Phys.* 14:477
69. Goldenfeld N. 1992. *Lectures on Phase Transitions and the Renormalization Group*. Reading, MA: Addison-Wesley
70. Sethna JP, Dahmen KA, Myers CR. 2001. Crackling noise. *Nature* 410:242–50
71. Csikor FF, Motz C, Weygand D, Zaiser M, Zapperi S. 2007. Dislocation avalanches, strain bursts, and the problem of plastic forming at the micrometer scale. *Science* 318:251–54
72. Friedman N, Jennings AT, Tsekenis G, Kim JY, Tao M, et al. 2012. Statistics of dislocation slip avalanches in nanosized single crystals show tuned critical behavior predicted by a simple mean field model. *Phys. Rev. Lett.* 109:095507
73. Burridge R, Knopoff L. 1967. Model and theoretical seismicity. *Bull. Seismol. Soc. Am.* 57:341–71
74. Bak P, Tang C. 1989. Earthquakes as a self-organized critical phenomenon. *J. Geophys. Res.* 94:635–15
75. Petri A, Paparo G, Vespignani A, Alippi A, Costantini M. 1994. Experimental evidence for critical dynamics in microfracturing processes. *Phys. Rev. Lett.* 73:3423
76. Garcimartin A, Guarino A, Bellon L, Ciliberto S. 1997. Statistical properties of fracture precursors. *Phys. Rev. Lett.* 79:3202
77. Chen Y, Papanikolaou S, Sethna JP, Zapperi S, Durin G. 2011. Avalanche spatial structure and multivariable scaling functions; sizes, heights, widths, and views through windows. *Phys. Rev. E* 84:061103
78. Papanikolaou S, Bohn F, Sommer RL, Durin G, Zapperi S, Sethna JP. 2011. Universality beyond power laws and the average avalanche shape. *Nat. Phys.* 7:316–20
79. Miguel MC, Vespignani A, Zapperi S, Weiss J, Grasso JR. 2001. Intermittent dislocation flow in viscoplastic deformation. *Nature* 410:667–71
80. Dimiduk DM, Woodward C, LeSar R, Uchic MD. 2006. Scale-free intermittent flow in crystal plasticity. *Science* 312:1188–90
81. Weiss J, Marsan D. 2003. Three-dimensional mapping of dislocation avalanches: clustering and space/time coupling. *Science* 299:99
82. Mughrabi H. 1983. Dislocation wall and cell structures and long-range internal stresses in deformed metal crystals. *Acta Metall.* 31:1367–79
83. Hähner P, Bay K, Zaiser M. 1998. Fractal dislocation patterning during plastic deformation. *Phys. Rev. Lett.* 81:2470
84. Hughes D, Chrzan D, Liu Q, Hansen N. 1998. Scaling of misorientation angle distributions. *Phys. Rev. Lett.* 81:4664
85. Chen YS, Choi W, Papanikolaou S, Bierbaum M, Sethna JP. 2013. Scaling theory of continuum dislocation dynamics in three dimensions: self-organized fractal pattern formation. *Int. J. Plast.* 46:94–129
86. Chen YS, Choi W, Papanikolaou S, Sethna JP. 2010. Bending crystals: the evolution of grain boundaries and fractal dislocation structures. *Phys. Rev. Lett.* 105:105501
87. Bertalan Z, Shekhawat A, Sethna JP, Zapperi S. 2014. Fracture strength: stress concentration, extreme value statistics, and the fate of the Weibull distribution. *Phys. Rev. Appl.* 2:034008
88. Kent-Dobias J, Shekhawat A, Sethna JP. 2016. Work in progress
89. Alava MJ, Nukala PK, Zapperi S. 2006. Morphology of two-dimensional fracture surfaces. *J. Stat. Mech. Theory Exp.* 2006:L10002
90. Zapperi S, Nukala PKV, Šimunović S. 2005. Crack roughness and avalanche precursors in the random fuse model. *Phys. Rev. E* 71:026106

91. Alava MJ, Nukala PK, Zapperi S. 2006. Statistical models of fracture. *Adv. Phys.* 55:349–476
92. Bouchaud E, Lapasset G, Planes J. 1990. Fractal dimension of fractured surfaces: a universal value? *EPL* 13:73
93. Bouchaud E. 1997. Scaling properties of cracks. *J. Phys. Condens. Matter* 9:4319
94. Ponson L, Bonamy D, Bouchaud E. 2006. Two-dimensional scaling properties of experimental fracture surfaces. *Phys. Rev. Lett.* 96:035506
95. Morel S, Schmittbuhl J, Bouchaud E, Valentin G. 2000. Scaling of crack surfaces and implications for fracture mechanics. *Phys. Rev. Lett.* 85:1678
96. Måløy KJ, Hansen A, Hinrichsen EL, Roux S. 1992. Experimental measurements of the roughness of brittle cracks. *Phys. Rev. Lett.* 68:213
97. Hansen A, Schmittbuhl J. 2003. Origin of the universal roughness exponent of brittle fracture surfaces: stress-weighted percolation in the damage zone. *Phys. Rev. Lett.* 90:045504
98. Schmittbuhl J, Hansen A, Batrouni GG. 2003. Roughness of interfacial crack fronts: stress-weighted percolation in the damage zone. *Phys. Rev. Lett.* 90:045505
99. Laurson L, Santucci S, Zapperi S. 2010. Avalanches and clusters in planar crack front propagation. *Phys. Rev. E* 81:046116
100. Schmittbuhl J, Roux S, Vilotte JP, Måløy KJ. 1995. Interfacial crack pinning: effect of nonlocal interactions. *Phys. Rev. Lett.* 74:1787
101. Rosso A, Krauth W. 2002. Roughness at the depinning threshold for a long-range elastic string. *Phys. Rev. E* 65:025101
102. Mecholsky J, Passoja D, Feinberg-Ringel K. 1989. Quantitative analysis of brittle fracture surfaces using fractal geometry. *J. Am. Ceram. Soc.* 72:60–65
103. Mecholsky J, Mackin T, Passoja D. 1988. Self-similar crack propagation in brittle materials. *Adv. Ceram.* 22:127–34
104. Mecholsky JJ, Freiman SW. 1991. Relationship between fractal geometry and fractography. *J. Am. Ceram. Soc.* 74:3136–38
105. Tsai Y, Mecholsky J. 1991. Fractal fracture of single crystal silicon. *J. Mater. Res.* 6:1248–63
106. Schmittbuhl J, Måløy KJ. 1997. Direct observation of a self-affine crack propagation. *Phys. Rev. Lett.* 78:3888
107. Schmittbuhl J, Schmitt F, Scholz C. 1995. Scaling invariance of crack surfaces. *J. Geophys. Res. Solid Earth* 100:5953–73
108. Schmittbuhl J, Gentier S, Roux S. 1993. Field measurements of the roughness of fault surfaces. *Geophys. Res. Lett.* 20:639–41
109. Santucci S, Måløy KJ, Delaplace A, Mathiesen J, Hansen A, et al. 2007. Statistics of fracture surfaces. *Phys. Rev. E* 75:016104
110. Chen YJ, Zapperi S, Sethna JP. 2015. Crossover behavior in interface depinning. *Phys. Rev. E* 92:022146
111. Talreja R, Weibull W. 1977. Probability of fatigue failure based on residual strength. In *Proceedings ICF4*. Oxford, UK: Pergamon Press
112. Jayatilaka AdS, Trustrum K. 1977. Statistical approach to brittle fracture. *J. Mater. Sci.* 12:1426–30
113. Phoenix SL, Taylor HM. 1973. The asymptotic strength distribution of a general fiber bundle. *Adv. Appl. Probab.* 5:200–16
114. Györgyi G, Moloney N, Ozogány K, Rácz Z, Droz M. 2010. Renormalization-group theory for finite-size scaling in extreme statistics. *Phys. Rev. E* 81:041135
115. Györgyi G, Moloney N, Ozogány K, Rácz Z. 2008. Finite-size scaling in extreme statistics. *Phys. Rev. Lett.* 100:210601
116. Salminen L, Tolvanen A, Alava MJ. 2002. Acoustic emission from paper fracture. *Phys. Rev. Lett.* 89:185503
117. Koivisto J, Rosti J, Alava MJ. 2007. Creep of a fracture line in paper peeling. *Phys. Rev. Lett.* 99:145504
118. Hemmer PC, Hansen A. 1992. The distribution of simultaneous fiber failures in fiber bundles. *J. Appl. Mech.* 59:909–14
119. Shekhawat A, Zapperi S, Sethna JP. 2013. From damage percolation to crack nucleation through finite-size criticality. *Phys. Rev. Lett.* 110:185505

120. Fisher DS. 1998. Collective transport in random media: from superconductors to earthquakes. *Phys. Rep.* 301:113–50
121. Zaiser M, Moretti P. 2005. Fluctuation phenomena in crystal plasticity: a continuum model. *J. Stat. Mech. Theory Exp.* 2005:P08004
122. Zaiser M. 2006. Scale invariance in plastic flow of crystalline solids. *Adv. Phys.* 55:185–245
123. Talamali M, Petäjä V, Vandembroucq D, Roux S. 2011. Avalanches, precursors, and finite-size fluctuations in a mesoscopic model of amorphous plasticity. *Phys. Rev. E* 84:016115
124. Durin G, Zapperi S. 2006. The Barkhausen effect. In *The Science of Hysteresis*, ed. G Bertotti, ID Mayergoyz, pp. 181–267. Oxford, UK: Academic Press
125. Narayan O, Fisher DS. 1993. Threshold critical dynamics of driven interfaces in random media. *Phys. Rev. B* 48:7030–42
126. Leschhorn H, Nattermann T, Stepanow S, Tang LH. 1997. Driven interface depinning in a disordered medium. *Ann. Phys.* 509:1–34
127. Chauve P, Giamarchi T, Le Doussal P. 2000. Creep and depinning in disordered media. *Phys. Rev. B* 62:6241–67
128. Chauve P, Le Doussal P, Wiese KJ. 2001. Renormalization of pinned elastic systems: How does it work beyond one loop? *Phys. Rev. Lett.* 86:1785–88
129. Le Doussal P, Wiese KJ, Chauve P. 2002. Two-loop functional renormalization group theory of the depinning transition. *Phys. Rev. B* 66:174201
130. Kagan YY. 2010. Earthquake size distribution: power-law with exponent $\beta = 1/2$? *Tectonophysics* 490:103–14
131. Ben-Zion Y. 2008. Collective behavior of earthquakes and faults: continuum-discrete transitions, progressive evolutionary changes, and different dynamic regimes. *Rev. Geophys.* 46:RG4006
132. Baró J, Corral A, Illa X, Planes A, Salje EKH, et al. 2013. Statistical similarity between the compression of a porous material and earthquakes. *Phys. Rev. Lett.* 110:088702
133. Fisher DS, Dahmen KA, Ramanathan D, Ben-Zion Y. 1997. Statistics of earthquakes in simple models of heterogeneous faults. *Phys. Rev. Lett.* 78:4885–88
134. Chen K, Bak P, Obukhov SP. 1991. Self-organized criticality in a crack-propagation model of earthquakes. *Phys. Rev. A* 43:625–30
135. Carlson JM, Langer JS. 1989. Properties of earthquakes generated by fault dynamics. *Phys. Rev. Lett.* 62:2632–35
136. Langer J, Carlson J, Myers CR, Shaw BE. 1996. Slip complexity in dynamic models of earthquake faults. *PNAS* 93:3825–29
137. Dahmen K, Ertaş D, Ben-Zion Y. 1998. Gutenberg-richter and characteristic earthquake behavior in simple mean-field models of heterogeneous faults. *Phys. Rev. E* 58:1494–501
138. Liu AJ, Nagel SR. 2010. The jamming transition and the marginally jammed solid. *Annu. Rev. Condens. Matter Phys.* 1:347–69
139. Liu AJ, Nagel SR, van Saarloos W, Wyart M. 2011. The jamming scenario—an introduction and outlook. In *Dynamical Heterogeneities in Glasses, Colloids, and Granular Media*, ed. L Berthier, G Biroli, J-P Bouchard, L Cipelletti, W van Saarloos, pp. 1–72. New York/Oxford, UK: Oxford Univ. Press
140. Ispánovity PD, Laurson L, Zaiser M, Groma I, Zapperi S, Alava MJ. 2014. Avalanches in 2D dislocation systems: Plastic yielding is not depinning. *Phys. Rev. Lett.* 112:235501
141. Bi D, Yang X, Marchetti MC, Manning ML. 2016. Motility-driven glass and jamming transitions in biological tissues. *Phys. Rev. X* 6:021011
142. Tsekenis G, Goldenfeld N, Dahmen KA. 2011. Dislocations jam at any density. *Phys. Rev. Lett.* 106:105501
143. Miguel MC, Vespignani A, Zaiser M, Zapperi S. 2002. Dislocation jamming and Andrade creep. *Phys. Rev. Lett.* 89:165501
144. Goodrich CP, Liu AJ, Sethna JP. 2016. Scaling ansatz for the jamming transition. *PNAS* 113:9745–50
145. Hatano T. 2008. Scaling properties of granular rheology near the jamming transition. *J. Phys. Soc. Jpn.* 77:123002
146. Tighe BP, Woldhuis E, Remmers JJC, van Saarloos W, van Hecke M. 2010. Model for the scaling of stresses and fluctuations in flows near jamming. *Phys. Rev. Lett.* 105:088303

147. Dinkgreve M, Paredes J, Michels MAJ, Bonn D. 2015. Universal rescaling of flow curves for yield-stress fluids close to jamming. *Phys. Rev. E* 92:012305
148. Nieh TG, Wadsworth J, Sherby OD. 2005. *Superplasticity in Metals and Ceramics*. Cambridge, UK: Cambridge Univ. Press
149. Pázmándi F, Zaránd G, Zimányi GT. 2000. Self-organized criticality in the hysteresis of the Sherrington–Kirkpatrick model. *Physica B Condens. Matter* 275:207–11
150. Lin J, Wyart M. 2016. Mean-field description of plastic flow in amorphous solids. *Phys. Rev. X* 6:011005
151. Dahmen KA, Ben-Zion Y, Uhl JT. 2009. Micromechanical model for deformation in solids with universal predictions for stress-strain curves and slip avalanches. *Phys. Rev. Lett.* 102:175501
152. Sun BA, Yu HB, Jiao W, Bai HY, Zhao DQ, Wang WH. 2010. Plasticity of ductile metallic glasses: a self-organized critical state. *Phys. Rev. Lett.* 105:035501
153. Antonaglia J, Wright WJ, Gu X, Byer RR, Hufnagel TC, et al. 2014. Bulk metallic glasses deform via slip avalanches. *Phys. Rev. Lett.* 112:155501
154. Liu C, Ferrero EE, Puosi F, Barrat JL, Martens K. 2016. Driving rate dependence of avalanche statistics and shapes at the yielding transition. *Phys. Rev. Lett.* 116:065501
155. Budrikis Z, Fernandez-Castellanos D, Sandfeld S, Zaiser M, Zapperi S. 2015. Universality of avalanche exponents in plastic deformation of disordered solids. arXiv:1511.06229 [cond-mat.mtrl-sci]
156. Salerno KM, Robbins MO. 2013. Effect of inertia on sheared disordered solids: critical scaling of avalanches in two and three dimensions. *Phys. Rev. E* 88:062206–15
157. Bak P, Tang C, Wiesenfeld K. 1988. Self-organized criticality. *Phys. Rev. A* 38:364–74
158. Rollett A, Humphreys F, Rohrer GS, Hatherly M. 2004. *Recrystallization and Related Annealing Phenomena*. Amsterdam: Elsevier
159. Csikor FF, Motz C, Weygand D, Zaiser M, Zapperi S. 2007. Dislocation avalanches, strain bursts, and the problem of plastic forming at the micrometer scale. *Science* 318:251–54
160. Zaiser M, Marmo B, Moretti P. 2005. The yielding transition in crystal plasticity—discrete dislocations and continuum models. In *Proceedings of the International Conference on Statistical Mechanics of Plasticity and Related Instabilities*, p. 53.1. Bangalore, Ind.: Ind. Inst. Sci.
161. Lehtinen A, Costantini G, Alava MJ, Zapperi S, Laurson L. 2016. Glassy features of crystal plasticity. *Phys. Rev. B* 94:064101
162. Papanikolaou S, Dimiduk DM, Choi W, Sethna JP, Uchic MD, et al. 2012. Quasi-periodic events in crystal plasticity and the self-organized avalanche oscillator. *Nature* 490:517–21
163. Jagla EA, Landes FP, Rosso A. 2014. Viscoelastic effects in avalanche dynamics: a key to earthquake statistics. *Phys. Rev. Lett.* 112:174301
164. Pázmándi F, Zaránd G, Zimányi GT. 1999. Self-organized criticality in the hysteresis of the Sherrington-Kirkpatrick model. *Phys. Rev. Lett.* 83:1034–37
165. Rutenberg AD, Vollmayr-Lee BP. 1999. Anisotropic coarsening: grain shapes and nonuniversal persistence. *Phys. Rev. Lett.* 83:3772–75
166. Shore JD, Holzer M, Sethna JP. 1992. Logarithmically slow domain growth in nonrandomly frustrated systems: Ising models with competing interactions. *Phys. Rev. B* 46:11376–404